Available online at www.sciencedirect.com

ScienceDirect

Nuclear Physics B 905 (2016) 16–44

NUCLEAR PHYSICS B

www.elsevier.com/locate/nuclphysb

Renormalization-group investigation of a superconducting U(r)-phase transition using five loops calculations

G.A. Kalagov [a,b], M.V. Kompaniets [a], M.Yu. Nalimov [a,*]

[a] *St. Petersburg State University, 7/9 Universitetskaya nab., St. Petersburg 199034, Russia*

[b] *Department of Theoretical Physics and Astrophysics, Faculty of Science, P.J. Safarik University, Park Angelinum 9, 041 54 Kosice, Slovak Republic*

Received 28 May 2015; received in revised form 1 February 2016; accepted 2 February 2016

Available online 5 February 2016

Editor: Hubert Saleur

Abstract

We have studied a Fermi system with attractive U(r)-symmetric interaction at the finite temperatures by the quantum field renormalization group (RG) method. The RG functions have been calculated in the framework of dimensional regularization and minimal subtraction scheme up to five loops. It has been found that for $r \geq 4$ the RG flux leaves the system's stability region – the system undergoes a first order phase transition. To estimate the temperature of the transition to superconducting or superfluid phase the RG analysis for composite operators has been performed using three-loops approximation. The result of this analysis shows that for $3D$ systems estimated phase transition temperature is higher then well known theoretical estimations based on continuous phase transition formalism.

* Corresponding author.

E-mail addresses: KalagovG@gmail.com (G.A. Kalagov), m.kompaniets@spbu.ru (M.V. Kompaniets), m.nalimov@spbu.ru (M.Yu. Nalimov).

http://dx.doi.org/10.1016/j.nuclphysb.2016.02.004

0. Introduction

The investigation of quantum Fermi systems and the phase transitions in these systems are the problems of permanent interest. To describe the quantum equilibrium Fermi system we use the temperature Green functions formalism, quantum field theory methods and the renormalization group approach. The analysis is based on the microscopic model with local attractive interaction of the "density–density" type [1–3]. The model's field action has the form

$$S_\psi = \psi^\dagger_\alpha(\partial_t - \frac{\Delta}{2m} - \mu)\psi_\alpha - \frac{\lambda}{2}\psi^\dagger_\alpha\psi^\dagger_\gamma\psi_\gamma\psi_\alpha, \tag{1}$$

where ψ_α, $\psi^\dagger_\alpha$ describe the fermion fields at the finite temperature T, these fields are complex-conjugate elements of the Grassmann algebra and $\alpha = 1, \dots, r$, where r is the number of spin degrees of freedom, Δ is Laplace operator; m is a mass of the particles; μ is the system's chemical potential; $\lambda = 4\pi|a_s|/m$ is positive coupling constant and a_s is the scattering amplitude for interparticle $3D$-scattering; t is the "imaginary" time and $t \in [0, \beta = 1/T]$. All the necessary integrations and summations in formula (1) and similar expressions below are implied. It is also necessary to impose the antiperiodic boundary conditions with respect to the "imaginary" time on the fermion fields.

$$\psi_\alpha(\mathbf{p}, 0) = -\psi_\alpha(\mathbf{p}, \beta), \quad \psi^\dagger_\alpha(\mathbf{p}, 0) = -\psi^\dagger_\alpha(\mathbf{p}, \beta). \tag{2}$$

In the $r = 2$ case, this action (1) corresponds to the Bardeen–Cooper–Schrieffer theory and $\alpha = \uparrow, \downarrow$ are the two possible spin projections. The theory describes low temperature superconductivity in electron systems. We will consider the case of arbitrary even values r. It can be corresponded to the systems of ultra-cold atoms with high spins: $3/2, 5/2, \dots, 9/2$, investigated recently [4–11] or with the electrons in a solid body which have an additional sublattice index, or layer index and/or an index correspondent to a degeneration of a zone structure. The modern example of such solid body is graphene [12], where electrons have two additional indexes connected both with the sublattices existence and the zone structure degeneration. The main part of our analysis is applied to the model of graphene with the density–density interaction. But for the graphene description the free-electron Hamiltonian in (1) has to be replaced to Dirac's one and the calculations in the Sec. 4 have to be repeated.

Usually in the system under consideration the phase transition temperature is determined by the appearance of the anomalous solution of the Dyson equation [1], and the order parameter of the superconducting phase transition is given by means of the composite operators $\langle\psi_\alpha\psi_\gamma\rangle$ and $\left\langle\psi^\dagger_\alpha\psi^\dagger_\gamma\right\rangle$. To investigate this model using renormalization group method, the action is transformed by introducing the new boson fields χ, $\chi^\dagger$ [14,15]. The action of the form

$$S_{\psi,\chi} = \psi^\dagger_\alpha(\partial_t + \varepsilon_\mathbf{p})\psi_\alpha + \frac{1}{2\lambda}\operatorname{tr}\chi\chi^\dagger - \frac{1}{2}\psi^\dagger_\alpha\chi_{\alpha\gamma}\psi^\dagger_\gamma - \frac{1}{2}\psi_\alpha\chi^\dagger_{\alpha\gamma}\psi_\gamma \tag{3}$$

was considered, where $\varepsilon_\mathbf{p} = \mathbf{p}^2/(2m) - \mu$.

It can be easily proven that the integration $\exp(-S_{\psi,\chi})$ over the fields χ, $\chi^\dagger$ leads to $\exp(-S_\psi)$. The new fields are complex skew-symmetric matrices because the fields ψ, $\psi^\dagger$ are Grassmann variables. The Schwinger equations

$$\langle\chi^\dagger_{\alpha\gamma} + \lambda\psi^\dagger_\alpha\psi^\dagger_\gamma\rangle = 0,$$
$$\langle\chi_{\gamma\alpha} - \lambda\psi_\alpha\psi_\gamma\rangle = 0.$$

show that the χ, $\chi^\dagger$ determine the order parameter of the phase transition.

The integration of $\exp(-S_{\psi,\chi})$ over the fermion fields ψ, $\psi^\dagger$ leads to the new action for the boson fields χ, $\chi^\dagger$

$$S_\chi = \frac{1}{2\lambda}\operatorname{tr}\chi\chi^\dagger - \operatorname{tr}\ln\begin{pmatrix} -\chi^\dagger & -i\omega_s - \frac{\Delta}{2m} - \mu \\ -i\omega_s + \frac{\Delta}{2m} + \mu & -\chi \end{pmatrix}, \tag{4}$$

where $\omega_s = \pi T(2s+1)$ are Matsubara frequencies, $s \in \mathbb{Z}$. Using the Taylor expansions for $\ln(1+\dots)$ we can rewrite the action as

$$S_\chi = \frac{1}{2\lambda}\operatorname{tr}\chi\chi^\dagger + \frac{1}{2}$$ 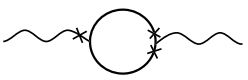 $$+ \frac{1}{4}$$  $$+\dots, \tag{5}$$

where wave lines denote the field χ, $\chi^\dagger$, the plain lines denote free $\langle\psi\psi^\dagger\rangle$ propagators, cross corresponds to $\psi^\dagger$, $\chi^\dagger$ fields.

To obtain the effective action in the infra red (IR) region we have to present (5) in the form of a Ginzburg–Landau functional by expanding all diagrams in the external momenta $\mathbf{p}$ and frequencies. Then $\chi^\dagger$, χ fields can be considered as t-independent. As a result the effective action has the form

$$S_\chi = \operatorname{tr}\chi^\dagger(c_0\mathbf{p}^2 + \widetilde{\tau}_0)\chi + \frac{\widetilde{g}_{01}}{4}\operatorname{tr}(\chi\chi^\dagger)\operatorname{tr}(\chi\chi^\dagger) + \frac{\widetilde{g}_{02}}{4}\operatorname{tr}(\chi\chi^\dagger\chi\chi^\dagger). \tag{6}$$

The term with $\widetilde{g}_{01}$ coupling constant has been included to obtain the multiplicatively renormalized theory. The parameters of the action c_0 and $\widetilde{g}_{02}$ are positive and can be calculated from the expressions

$$\widetilde{g}_{01} = 0, \quad \widetilde{g}_{02} = \beta T\sum_{\omega_s}\int\frac{d^D\mathbf{k}}{(2\pi)^D}\frac{1}{(\omega_s^2+\varepsilon_\mathbf{k}^2)^2},$$
$$\widetilde{\tau}_0 = \frac{\beta}{2\lambda} - \frac{\beta}{2}T\sum_{\omega_s}\int\frac{d^D\mathbf{k}}{(2\pi)^D}\frac{1}{\omega_s^2+\varepsilon_\mathbf{k}^2}, \tag{7}$$

$$c_0 = -\frac{\beta}{2}T\partial_\mathbf{p}^2\sum_{\omega_s}\int\frac{d^D\mathbf{k}}{(2\pi)^D}\frac{1}{(i\omega_s+\varepsilon_\mathbf{k})(-i\omega_s+\varepsilon_{\mathbf{k}+\mathbf{p}})}\bigg|_{\mathbf{p}=0}, \tag{8}$$

where D is dimension of space. The integration over $\mathbf{k}$ is performed in a narrow neighborhood of the Fermi surface $|\varepsilon_\mathbf{k} - \mu| < \delta$. The parameter δ can be similar to Debye frequency ω_D for the system of electrons in the solids or similar to Fermi energy ε_F for ultra cold atom systems. For such systems $\delta = (2/e)^{7/3}\varepsilon_F \approx 0.49\varepsilon_F$ [13].

The IR behavior of the model (6) was studied in [14,15]. The renormalization group (RG) investigation in the framework of $\varepsilon = 4 - D$ expansion in one-loop approximation [14] and then in three-loop approximation [15] establishes the absence of IR-stable fixed points for even values of $r \geq 4$. It was found that the stability criterion for action (6) (the condition for positive definiteness of an interaction) can be formulated as the inequality

$$g_2 + rg_1 > 0, \tag{9}$$

for $g_2 > 0$.

Moreover, solutions of the RG equations for the invariant charges in one-loop approximation [14] show that the system loses the stability before the continuous phase transition occurs. It

was supposed, that a first-order phase transition takes place here and this phase transition can be considered as one of the possible reasons of high temperature superconductivity.

Then the similar behavior was confirmed in [15] in the three-loop RG analysis of the 3D and 2D models. But it was found that the three-loop approximation is not sufficient to ensure an accurate calculation of the phase transition temperature. Therefore we have to develop our analysis up to five-loop calculations, which is the maximal order available now in the framework of ε-expansion [19].

In Sec. 1 we describe the five-loop RG analysis of the model investigated with $r \geq 4$. According to [14] there is no IR stable fixed point in the framework of ε expansion. Thus, instead of seeking fixed points of the RG equation we restrict ourselves to the analysis of the phase trajectories. It was indicated in [14] that the equations for the invariant charges can be constructed in the ε-expansion form.

To analyze the phase portrait of these equations in the physical space dimensions ($\varepsilon = 1$, $\varepsilon = 2$) we must resum the terms calculated using, for instance, the Borel resummation technique. Such a resummation requires knowing the higher orders asymptotics (HOA) of the ε expansion. The HOA of the considered model was determined in [15] using methods of the instanton analysis [17]. The analysis and the results obtained are described briefly in Sec. 2. It is interesting to note that we have found several instantons with different matrix structures. These instantons are essential in a Borel resumming at different values of the charges g_1, g_2.

In Sec. 3 we resum and solve numerically the RG equations for the invariant charges. It is confirmed that the invariant charges in the $3D$ model cross the boundary (9) of the stability domain of the action (6). As for the $2D$ model, it is found that five-loop approximation is not sufficient yet for the accurate description of the phase transition type. Our results show that the phase transition type depends on the initial value of the coupling constant g_{20}.

In Sec. 4 the first order phase transition is studied in $3D$ and $2D$ model to find the real phase transition temperature. The additional terms ($\sim \chi^6$) are introduced in the action (6). These terms are IR irrelevant for the critical behavior, but are relevant for the first order phase transition description. They are renormalized as composite operators in three-loop approximation. Their contributions to the state equation are Borel resummed and the phase transition temperature is estimated.

1. Renormalization group analysis

The renormalized action of the considered model is given by the expression [14]

$$S_R = Z_\chi^2 \operatorname{tr} \chi^\dagger(-\Delta)\chi + Z_\tau Z_\chi^2 \tau \operatorname{tr} \chi^\dagger \chi + Z_{g_1} Z_\chi^4 M^\varepsilon \frac{g_1}{4} \left(\operatorname{tr} \chi \chi^\dagger\right)^2 + Z_{g_2} Z_\chi^4 M^\varepsilon \frac{g_2}{4} \operatorname{tr} \chi \chi^\dagger \chi \chi^\dagger. \tag{10}$$

This expression is obtained by the multiplicative renormalization

$$g_{0j} \to g_j M^\varepsilon Z_{g_i}, \quad \chi \to \chi Z_\chi, \quad \tau_0 \to \tau Z_\tau, \tag{11}$$

where the parameter M is a so-called renormalization mass; g_1, g_2 are dimensionless renormalized coupling constants, index zero denotes bare parameters. In this paper we use the dimensional regularization, the ε-expansion and the minimal subtraction scheme (MS-scheme) [16]. The bare parameters g_{0j} and τ_0 are associated with the microscopic parameters (7), (8) by the relations $g_{0j} = \widetilde{g}_{0j}/c_0^2$, $\tau_0 = \widetilde{\tau}_0/c_0$ and $\chi \to \chi/\sqrt{c_0}$.

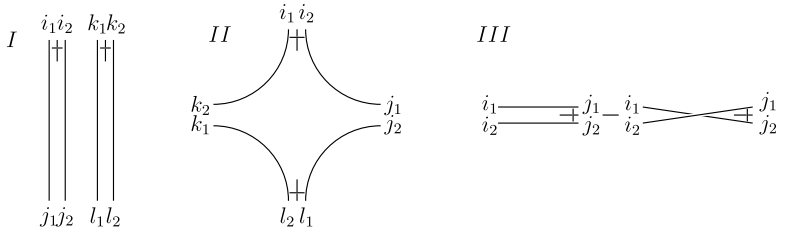

Fig. 1. Tensor structures of the vertices and propagator: vertex I corresponds to g_1, vertex II corresponds to g_2, and vertex III corresponds to the propagator.

Let us introduce the basic elements of the Feynman diagrammatic techniques for the model. In the momentum representation the free propagator has the form

$$\Pi^{j_1 j_2}_{i_1 i_2} = \frac{W^{j_1 j_2}_{i_1 i_2}}{\mathbf{k}^2 + \tau_0} \quad \text{and} \quad W^{j_1 j_2}_{i_1 i_2} \equiv \frac{1}{2}(\delta_{i_1 j_1}\delta_{i_2 j_2} - \delta_{i_1 j_2}\delta_{i_2 j_1}),$$

where δ_{ij} is Kronecker symbol; $\mathbf{k}$ is the momentum or the wave vector ($\hbar = 1$). The tensor $W^{j_1 j_2}_{i_1 i_2}$ is antisymmetric with respect to the transpositions of its indexes $i_1 \leftrightarrow i_2$ and $j_1 \leftrightarrow j_2$, and symmetric with respect to the transposition of the pairs $(i_1, i_2) \leftrightarrow (j_1, j_2)$. One can write the tensor structures for the vertices g_1 and g_2 too, but we give only their graphical representation (Fig. 1), the vertices antisymmetrization is implied.

In MS-scheme all renormalization constants have the form of the poles in ε

$$Z_e = 1 + \frac{Z^1_e}{\varepsilon} + O\left(\frac{1}{\varepsilon^2}\right), \quad e = (g_j, \tau, \chi)$$

where $Z^1_e(g_1, g_2)$ denotes the residue at the simple pole in ε for the corresponding renormalization constant. Let us remark that the interaction $\left(\mathrm{tr}\,\chi\chi^\dagger\right)^2$ must be included for the multiplicative renormalizability of the theory. It is easy to verify that the corresponding counterterms appear due to the renormalization of the theory starting with the simplest one-loop diagram.

The RG-functions (the coefficients of the RG equation [16]) are defined by the relations

$$\beta_{g_j} = \widetilde{D}_M Z_{g_i}, \quad \gamma_e = \widetilde{D}_M \ln Z_e, \tag{12}$$

where $\widetilde{D}_M$ is the differential operator $M\partial_M$ at fixed bare parameters, β_{g_j} are beta-functions of the charges g_i, and the functions γ_e are anomalous dimensions for the parameters e. In the MS-scheme the RG-functions are connected with the renormalization constants by the following expressions [16]

$$\beta_{g_j} = -g_j(\varepsilon + \gamma_{g_j}), \quad \gamma_e = -g_k \partial_k Z^1_e. \tag{13}$$

Program "FORM" [18] was used for the tensor structure calculations of the graphs. Tensor structure of the graph can be factorized, and the rest of the diagram is equivalent to diagrams of the scalar Φ^4 model, the values for these diagrams are taken from well known five loop calculations of the $O(n)$-symmetric Φ^4 model [19,20].

Finally, in the five-loop approximation (about 120 000 diagrams), the RG-functions of the theory were calculated. The rescale of the charges $g_i \to g_i/16\pi^2$ was used. Results of our calculations were controlled for $r = 2$, $r = 3$. In these cases the model (10) is equivalent to the $O(2)$- and $O(6)$–Φ^4 models with vector order parameter, respectively.

The RG equation leads to the known equations for the invariant coupling constants

$$\partial_\xi \bar{g}_i = \frac{\beta_{g_i}}{2+\gamma_\tau}, \quad \bar{g}_i|_{\xi=0} = g_i, \quad \text{where} \quad \xi \equiv \ln\frac{\tau}{M^2}. \tag{14}$$

The infrared (IR) regime $\xi \to -\infty$ is usually connected with fixed points (g_1^*, g_2^*) that are determined by the conditions $\beta_{g_i}(g_1^*, g_2^*) = 0$ for all indices i. The fixed point is IR-stable, if the matrix $\omega_{ij} \equiv \partial_{g_j}\beta_{g_i}(g_1^*, g_2^*)$ is positively defined. However, in the one-loop approximation [14] it was found, that these points do not exist for $r \geq 4$. There is the IR-stable fixed point in the model at $r = 2$, this point describes the critical behavior of the superconducting phase transition in systems with 1/2-spin fermions. Also, the model (10) has the IR-stable fixed point at $r = 3$. We will not try to determine the possible fixed point in the five-loops approximation of the model considered, instead of this trajectories of the invariant charges will be studied in the next sections.

2. Instanton analysis

Consider the equations (14) with the β-functions (49), (50) (see Appendix). After the scaling of the charges $\bar{g}_i$ and the dynamical variable of the RG equation ξ as $\bar{g}_i \to \varepsilon\bar{g}_i$ and $\xi \to \xi/\varepsilon$, we get eq. (14) in the form

$$\begin{aligned} &\partial_\xi \bar{g}_i = -\bar{g}_i + \sum_{N=0}^{K} \varepsilon^N B_i^{(N)}(\bar{g}_1, \bar{g}_2), \quad i = 1, 2 \\ &\bar{g}_i|_{\xi=0} = g_i. \end{aligned} \tag{15}$$

Explicit expressions of the $B_i^{(N)}(\bar{g}_1, \bar{g}_2)$ can be obtained from (49), (50). In our case $K = 4$ (five-loop approximation). Equations (15) can be solved in the form of ε-expansion with the formally small parameter ε. Similar to [14] we will consider numerical solution of the equations (15). As usual, the ε-expansion in the right hand side of equations (15) is an asymptotic expansion with zero radius of convergence. Therefore the equations (15) must be resummed to obtain results at physical points $\varepsilon = 1$ or $\varepsilon = 2$. The resummation process requires knowledge about the asymptotic behavior of $B_i^{(N)}(\bar{g}_1, \bar{g}_2)$ at $N \to \infty$. Such an asymptotic behavior is called a higher-order asymptotic (HOA) and was investigated in [15] in the model considered.

Let us recall the main details of the analysis [15]. The investigation of the asymptotic behavior of higher-order perturbation corrections proposed in [17] is based on the saddle-point expansion of the path integral (instanton approach). Calculation method for the HOA of renormalization constants in MS scheme developed in [22,21] was used.

Partially renormalized Green functions, where subtractions of all the divergences in subgraphs up to order $N-1$ are supposed, were considered. The coefficients $G_{2k}^{(N)}$ of the expansion in the parameter ε of the $2k$-point Green function

$$\begin{aligned} &G_{2k}(\varepsilon, x_1, \ldots, x_{2k}) = W^{-1} \int \mathcal{D}\chi\mathcal{D}\chi^\dagger \chi(x_1)\chi(x_2)^\dagger \ldots \chi(x_{2k-1})\chi(x_{2k})^\dagger e^{-S_R}, \\ &W = \int \mathcal{D}\chi\mathcal{D}\chi^\dagger e^{-S_R} \end{aligned} \tag{16}$$

can be calculated in high orders ($N \to \infty$) by the saddle-point method in the integral representation [17]

$$G_{2k}^{(N)}(x_1, \ldots, x_{2k}) = \frac{(-1)^N}{2\pi i} \oint\limits_\gamma \frac{d\varepsilon G_{2k}(\varepsilon, x_1, \ldots, x_{2k})}{(-\varepsilon)^{N+1}}, \tag{17}$$

where γ is a closed contour encircling the origin in the complex plane of ε. As usual [17], we will find the HOA at $\tau = 0$ and $D = 4$. After the rescaling of the parameters $g_i \to g_i/N$, $\chi \to \sqrt{N}\chi$, $\chi^\dagger \to \sqrt{N}\chi^\dagger$ the variational equations for functional $S_R + \ln(-\varepsilon)$ with respect to the field variables and ε take the form

$$
\begin{aligned}
&-\Delta\chi + \frac{\varepsilon g_1}{2}\chi \operatorname{tr}\chi\chi^\dagger + \frac{\varepsilon g_2}{2}\chi\chi^\dagger\chi = 0,\\
&-\Delta\chi^\dagger + \frac{\varepsilon g_1}{2}\chi^\dagger \operatorname{tr}\chi\chi^\dagger + \frac{\varepsilon g_2}{2}\chi^\dagger\chi\chi^\dagger = 0,\\
&\int d\mathbf{x}\left\{\frac{\varepsilon g_1}{4}\left(\operatorname{tr}\chi\chi^\dagger\right)^2 + \frac{\varepsilon g_2}{4}\operatorname{tr}\chi\chi^\dagger\chi\chi^\dagger\right\} = -1.
\end{aligned}
\tag{18}
$$

Similar to [17], the counterterms $Z_e - 1$ in the action (10) are irrelevant for the calculation of the stationary points. For matrix fields χ, $\chi^\dagger$ we can assume, without loss of generality, the block-diagonal Pfaff's form consisting of $p = r/2$ blocks

$$
\chi = \operatorname{diag}(s_1\sigma, \ldots, s_p\sigma), \quad \chi^\dagger = -\operatorname{diag}(s_1^*\sigma, \ldots, s_p^*\sigma), \quad \sigma = \begin{pmatrix} 0 & -1 \\ 1 & 0 \end{pmatrix},
\tag{19}
$$

with some complex functions $s_j(\mathbf{x})$. Any skew-symmetric matrix can be reduced to this form by some unitary transformations $U(r)$. The equations (18) and (19) yield the system of equations for $s_j(\mathbf{x})$

$$
-\Delta s_i(\mathbf{x}) + \varepsilon g_1 \sum_{k=1}^{p} |s_k(\mathbf{x})|^2 s_i(\mathbf{x}) + \frac{\varepsilon g_2}{2}|s_i(\mathbf{x})|^2 s_i(\mathbf{x}) = 0.
\tag{20}
$$

We seek $s_j(\mathbf{x})$ in the form

$$
s_i(\mathbf{x}) = \frac{\alpha_i\, y^{-1}}{|\mathbf{x} - \mathbf{x}_0|^2 + y^2}, \quad \alpha_i \in \mathbb{C},
\tag{21}
$$

similar to solutions of the variational equation for the scalar Φ^4 model. Functions $s_i(\mathbf{x})$ depend on $\mathbf{x}_0$ and y-arbitrary parameters reflecting the translation and dilatation invariance of the theory. Then the Faddeev–Popov method was used. The unit decomposition was inserted in the integrand (17) similar to [17]. This decomposition contains δ functions which fix $\mathbf{x}_0 = 0$, y, the complex phases and the Pfaff's form for the solutions of the (18). It is well known that this approach gave us an opportunity to eliminate the zero-modes problem [17] and it is essential for the calculation of the amplitudes of the Green function's HOA. But these amplitudes do not contribute to the resummation procedure described below. The only essential contribution from the unit decomposition is the exponent of N which can be simply determined by the knowledge about the number of zero-modes. For this reason we omit the rather cumbersome explicit expressions for the unit decomposition used. Substituting (21) in (20), we get the system of algebraic equations for constants α_i

$$
8\,\alpha_i + \varepsilon g_1 \sum_{k=1}^{p} |\alpha_k|^2\alpha_i + \frac{\varepsilon g_2}{2}|\alpha_i|^2\alpha_i = 0.
\tag{22}
$$

One can see that the stationary solutions may contain $m = 0, \ldots, p-1$ zero blocks with $|\alpha_i| = 0$ and $n = p, \ldots, 1$ blocks with $|\alpha_i|^2 = -16/(2n\varepsilon g_1 + \varepsilon g_2)$, and $n + m = p$.

Combining the instanton solutions (21), the Pfaff's form (19) and the third equation (18), we get stationary point in ε parameter as

$$\varepsilon_{st}(n) = -\frac{4n}{3}\frac{1}{2ng_1 + g_2}. \tag{23}$$

Then one can obtain the HOA of four-point Green functions expansions. The problem of connections between HOA of Green functions and HOA of renormalization constants in MS scheme is rather difficult, but it was discussed in [22,23]. Here we will use the result obtained without cumbersome explanations. Let us note that we are interested in the HOA of the renormalization constants Z_{gi}, namely HOA of the first(simple) pole in $N\epsilon$. The main terms of the latter are practically the same as the HOA of the four-point Green function obtained from (17) using (23). Thus (23) determines the $(-a)^N$ term in the expression below, but the b_0 according to [22,23] is dependent on the zero-modes number only. Then using (13), the beta-functions HOA can be obtained in the form

$$\beta_i^{(N)}(g_1, g_2) = const_i\, N! N^{b_n}\, (-a)^N \left(1 + O\left(N^{-1}\right)\right), \tag{24}$$

where $const_i$ – some constants not essential for future analysis, $b_n = (r^2 - 2r + n + 11)/2$ and $a = \max_n |a(n)|$, $a(n) = -1/\varepsilon_{st}(n)$. One can see from (23), that $a(n)$ depends on values of g_i, therefore the largest of all $a(n)$ gives the largest contribution to the HOA. Thus the perturbation series in the parameter ε have zero radius of convergence in the theory with the action (10). For this reason, it is necessary to use some procedures of resummation e.g. the Borel method.

3. Solution of the RG equations

3.1. Resummation of the RG equations

Let us recall the basic expressions for the Borel resummation [25]. We assume that there is a function $Q(\varepsilon)$ defined as a series in the parameter ε

$$Q(\varepsilon) = \sum_{N\geq 0} \varepsilon^N Q^{(N)}, \tag{25}$$

and the higher-order asymptotics of the series coefficients are determined by expression (24). The Borel transform of the series (25) is given by the relations

$$Q(\varepsilon) = \int_0^\infty dt\; e^{-t} t^{b_0} B(\varepsilon t), \quad B(t) = \sum_{N\geq 0} B^{(N)} t^N, \quad B^{(N)} = \frac{Q^{(N)}}{\Gamma(N + b_0 + 1)}, \tag{26}$$

where b_0 is an arbitrary parameter. The known asymptotic expansion (24) together with several assumptions about the analytic properties of $B(t)$ allow one to resum series (25) using (26) and to obtain a more precise value of $Q(\varepsilon)$. According to (24), the series $B(t)$ given by (26) converges in the circle $|t| < 1/a$, because $B^{(N)} \sim (-a)^N N^{b_n - b_0}$ as $N \to \infty$. The nearest singularity of the series is located on the negative real half-axis at the point $t = -1/a$. Then the integration contour over $t \in [0, +\infty)$ intersects the boundary of the circle of convergence for expression (25) at the point $1/a$. The problem of analytical continuation of (26) beyond the convergence domain $|t| < 1/a$ can be solved either by the method of the conformal mapping of the complex plane or by Padé approximation method [25]. Below we will use the conformal mapping method, because

it is controlled by HOA. Furthermore, it leads to more accurate results than other methods (see [26]). In our case the position of the $B(t)$-function poles depends on the position of the invariant coupling constants in the $(\bar{g}_1, \bar{g}_2)$ plane.

For example, let us consider a system (14) with $r = 4$. There are two kinds of instantons in the model. For instanton containing one non-zero block we get $a(1) = 3(2g_1 + g_2)/4$. Otherwise, instanton has two non-zero blocks and $a(2) = 3(4g_1 + g_2)/8$. Therefore in stability sector (9) there are two regions in the plane $(\bar{g}_1, \bar{g}_2)$ where series for $B(t)$ have different analytical properties:

Region I: if the invariant coupling constants satisfy the condition $8\bar{g}_1 + 3\bar{g}_2 > 0$, then $|a(1)| > |a(2)|$. The nearest singularity of the $B(t)$ is $t = -1/a(1)$;

Region II: if the invariant coupling constants satisfy the condition $8\bar{g}_1 + 3\bar{g}_2 \leq 0$, then $|a(2)| > |a(1)|$. In this case the nearest singularity of the $B(t)$ is located on the positive real half-axis at the point $t = 1/|a(2)|$.

Thus, the plane $(\bar{g}_1, \bar{g}_2)$ is divided by the line $8\bar{g}_1 + 3\bar{g}_2 = 0$. Above this boundary the analytical properties of $B(t)$-functions are determined by one non-zero block instanton, under the boundary only the two non-zero blocks instanton influences the properties of the function $B(t)$.

The initial values of the invariant coupling constants are located in the region I. Let us apply conformal mapping method to the equations (15) for invariant coupling constants located in this region. Usually the conformal map of the complex plane is chosen in the form [24,25]

$$u(\varepsilon) = \frac{\sqrt{1 + a\varepsilon} - 1}{\sqrt{1 + a\varepsilon} + 1} \quad \Leftrightarrow \quad \varepsilon(u) = \frac{4u}{a(u-1)^2}. \tag{27}$$

The series (25) can be rewritten in terms of the variable u as

$$B(\varepsilon) = \sum_{N \geq 0} B^{(N)} \varepsilon^N = \sum_{N \geq 0} U^{(N)} u^N,$$

$$U^{(0)} = B^{(0)}, \quad U^{(N)} = \sum_{m=1}^{N} B^{(m)} (4/a)^m C_{N+m-1}^{N-m}, \quad N \geq 1, \tag{28}$$

then the conformal Borel map of the quantity Q looks as follows

$$Q(\varepsilon) = \sum_{N \geq 0} U^{(N)} \int_0^\infty dt\, t^{b_0} e^{-t} u(\varepsilon t)^N. \tag{29}$$

Usually, the parameter b_0 is chosen to weaken the singularity of the Borel transform (26) at the point $t = -1/a$. It is fixed by the relation $b_0 = b_n + 3/2$ [24,25].

In the region II the singularity of the function $B(t)$ is located on the positive real half-axis, thus the conformal mapping method cannot be used.

3.2. Numerical analysis of the RG-equations

Combining the RG equations (15) and resummation formula (29), we have resummed the RG equations for the invariant coupling constants

$$\partial_\xi \bar{g}_i = -\bar{g}_i + \sum_{N=0}^{K} U_i^{(N)} \int_0^\infty dt\, t^{b_0} e^{-t} u(\varepsilon t)^N,$$

$$\bar{g}_i|_{\xi=0} = g_i. \tag{30}$$

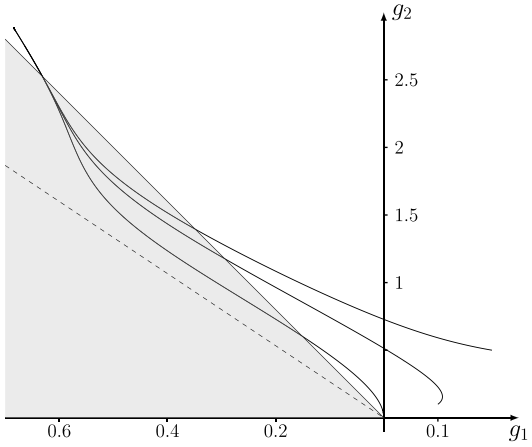

Fig. 2. Trajectories of the running coupling constants at $D = 3$ and $r = 4$; dashed line – the boundary of applicability of the resummation method.

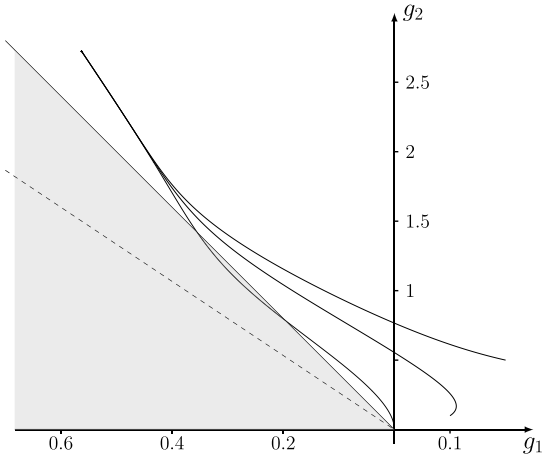

Fig. 3. Trajectories of the running coupling constants at $D = 2$ and $r = 4$; dashed line – the boundary of applicability of the resummation method.

Note that $U_i^{(N)}$ and $u(t)$ are functions of the variables $\bar{g}_i$. This system of equations (30) can be solved by the standard finite-difference method.

The results of the numerical solutions of the system (30) for $r = 4$ are shown as an example in Fig. 2 at $\varepsilon = 1$ and Fig. 3 at $\varepsilon = 2$. Fig. 2 shows that in a three dimensional model the invariant charges trajectories starting with different initial values cross the boundary of the action stability domain at some value ξ_0 of the parameter ξ. Similar behavior is observed for different values $r \geq 4$.

Fig. 4 shows how the trajectories of the invariant charges depend on the order of loops calculations for $D = 3$. We can state that five-loops approximation is sufficient to ensure the loss of the action stability and accurate calculation of ξ_0. Moreover, numerical analysis shows that solutions of the Cauchy problem (30) are stable under small perturbations of initial conditions.

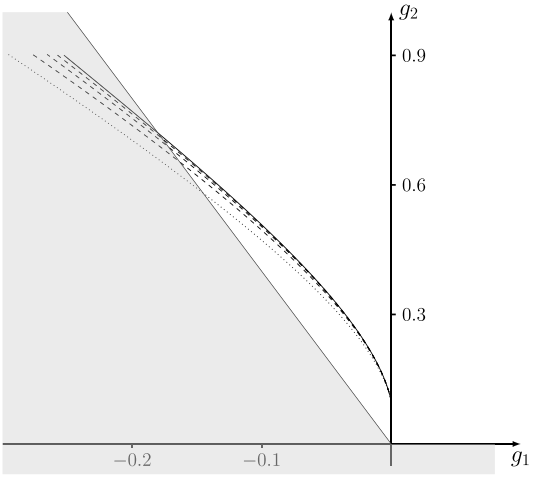

Fig. 4. The solutions of the RG equations ($D = 3, r = 4$) at different numbers of calculated loops: 1-loop – dotted line, 5-loops – solid line.

It is interesting to note, that we have found the IR stable fixed point of RG equation. According to [14,15] there is no IR stable fixed point for β-functions in one, two and three-loops approximations. The fixed point appears in four-loops. But the five-loops corrections essentially change the position of this fixed point, so we can guarantee neither existence nor position of this fixed point.

In $D = 2$ ($\varepsilon = 2$) case the IR stable fixed point is found in four- and five-loop approximation too. But in difference to three-loops ones [15] only rare trajectories of the invariant charges cross the line of the action stability (9) according to Fig. 3. These trajectories are connected with the very small initial values of renormalized coupling constants.

Our calculations are valid if the invariant coupling constants are in the region I. In the region II the series cannot be resummed by the Borel method. Finally, note that $a(1)$ gives the largest contribution to the HOA in the stability domain and in the neighborhood of the stability boundary for any $r > 2$. One can assume that the phase transition occurs near the boundary of stability. For this reason resummation process can be made only for $a(1)$.

4. The phase transition description

The loss of the action stability is usually considered as a mark of the first-order phase transition. But obviously, it is not possible to claim that ξ_0 defines the first-order phase transition temperature; only metastable states appear in the system at $\xi = \xi_0$. To answer the question when the new state of the system (with a condensate) in fact becomes stable, i.e., to determine the phase transition temperature, more accurate analysis is necessary.

Because the interaction terms ($\sim \chi^4$) of the action (10) are not positively defined now, we have to take into account the next term ($\sim \chi^6$) of the "bubble" expansion of the action (5).

Let us consider the effective action (10) with an additional $F_3 \equiv \mathrm{tr}(\chi^\dagger \chi)^3$ term. In the renormalization procedure in $4 - \varepsilon$ scheme F_3 will be considered as a composite operator of canonical dimension $\Delta_3 = 6 - 3\varepsilon$. Also, there are composite operators $F_2 \equiv \mathrm{tr}(\chi^\dagger \chi)^2\,\mathrm{tr}(\chi^\dagger \chi)$ and $F_1 \equiv (\mathrm{tr}\,\chi^\dagger \chi)^3$ with the same canonical dimension as F_3, therefore they may be mixed in the process of renormalization. Thus the term $\lambda_{0j} F_j/36$ must be included in the effective action,

here λ_{0j} are bare homogeneous sources. One can define the set of renormalized parameters λ_i using $\lambda_{0j} = Z_{jk}\lambda_k M^{2\varepsilon-2}$, for such extended model $Z_{jk} = \delta_{jk} + Z^1_{jk}/\varepsilon + O(1/\varepsilon^2)$. Matrix Z is a function of the variables g_i. Similar to the (13) we can write RG functions for λ_j

$$\beta_{\lambda_j} = -(2\varepsilon - 2)\lambda_j + \lambda_i g_k \frac{\partial}{\partial g_k} Z^1_{ij}. \tag{31}$$

One-loop approximation of matrix Z leads to the following results (corresponding three loop beta functions are presented in Appendix)

$$\beta_{\lambda_1} = 2(1-\varepsilon)\lambda_1 + g_1\left[\frac{3}{4}\lambda_1(r^2 - r + 14) + \lambda_2(r-1) + \frac{3}{4}\lambda_3\right] + \frac{3}{2}g_2\left[\lambda_1(r-1) + \lambda_2\right], \tag{32}$$

$$\beta_{\lambda_2} = 2(1-\varepsilon)\lambda_2 + \frac{1}{4}g_1\left[\lambda_3(6r-9) + \lambda_2(r^2 - r + 38)\right] + \frac{3}{2}g_2\left[6\lambda_1 + \lambda_2(r-2) + 3\lambda_3\right], \tag{33}$$

$$\beta_{\lambda_3} = 2(1-\varepsilon)\lambda_3 + \frac{15}{2}g_1\lambda_3 + \frac{3}{2}g_2\left[\lambda_3(r-4) + 4\lambda_2\right], \tag{34}$$

the rescaling of charges $g_i \to g_i/16\pi^2$ is assumed.

Let us mark that the full family of the composite operators with the same canonical dimension in the $D = 4$ dimensional space must be taken into account for an accurate calculation of the F_i operators renormalization.

This family also includes the operators

$$\begin{aligned}
&f_2 = \mathrm{tr}(\Delta\chi^+\Delta\chi), \quad f_{41} = \mathrm{tr}(\Delta\chi^+\chi\chi^+\chi) + \mathrm{tr}(\chi^+\Delta\chi\chi^+\chi),\\
&f_{42} = \mathrm{tr}(\partial_i\chi^+\chi\partial_i\chi^+\chi) + \mathrm{tr}(\chi^+\partial_i\chi\chi^+\partial_i\chi),\\
&f_{43} = \mathrm{tr}(\Delta\chi^+\chi)\,\mathrm{tr}(\chi^+\chi) + \mathrm{tr}(\chi^+\Delta\chi)\,\mathrm{tr}(\chi^+\chi),\\
&f_{44} = \mathrm{tr}(\partial_i\chi^+\chi)\,\mathrm{tr}(\partial_i\chi^+\chi) + \mathrm{tr}(\chi^+\partial_i\chi)\,\mathrm{tr}(\chi^+\partial_i\chi),\\
&f_{45} = \mathrm{tr}(\partial_i\chi^+\partial_i\chi)\,\mathrm{tr}(\chi^+\chi)
\end{aligned} \tag{35}$$

in addition to the F_i operators. The canonical dimensions of these operators are $d[f_2] = D + 2$, $d[f_{4i}] = 2D - 2$. But in the analysis presented we limit ourselves by the consideration of the F_i operators only. The contributions of the operators (35) will be discussed below.

It was shown in [14] that $\langle\chi\rangle$ is an order parameter of the phase transition in the model considered. A non-zero value of $\langle\chi\rangle$ leads the superfluid phase transition. The value for magnitude $\langle\chi\rangle$ can be calculated by minimization of the free energy $-\Gamma$. In the framework of the Landau mean field theory this functional can be written in the form

$$-\Gamma = \tau\,\mathrm{tr}\,\langle\chi\rangle^\dagger\langle\chi\rangle + \frac{g_{01}}{4}\left(\mathrm{tr}\,\langle\chi\rangle\langle\chi\rangle^\dagger\right)^2 + \frac{g_{02}}{4}\,\mathrm{tr}\,\langle\chi\rangle\langle\chi\rangle^\dagger\langle\chi\rangle\langle\chi\rangle^\dagger + \frac{\lambda_{01}}{36}\left(\mathrm{tr}\,\langle\chi\rangle\langle\chi\rangle^\dagger\right)^3 + \frac{\lambda_{02}}{36}\,\mathrm{tr}\left(\langle\chi\rangle\langle\chi\rangle^\dagger\right)^2\mathrm{tr}\,\langle\chi\rangle\langle\chi\rangle^\dagger + \frac{\lambda_{03}}{36}\,\mathrm{tr}\left(\langle\chi\rangle\langle\chi\rangle^\dagger\right)^3. \tag{36}$$

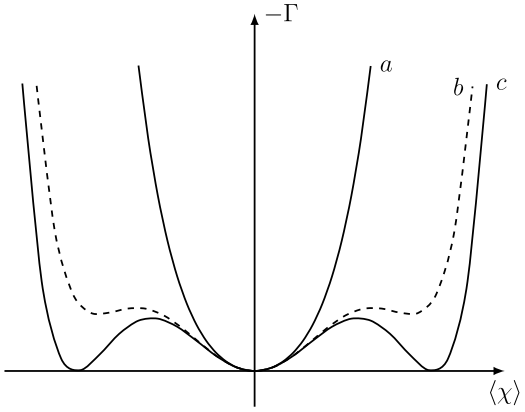

Fig. 5. Thermodynamics potential as a function of order parameter: a – disorder state, b – metastable state, c – "superfluid" state.

Schematically it can be represented in the figure Fig. 5. The variables $\langle\chi\rangle$ and $\langle\chi\rangle^{\dagger}$ have the Pfaffian form (19). For the extrema conditions at the phase transition pointwe get

$$\frac{\partial}{\partial\langle\chi\rangle_j}\Gamma=0,\quad \frac{\partial}{\partial\langle\chi\rangle_j^*}\Gamma=0,\quad \Gamma=0,\quad \forall j=0,\dots,r/2. \tag{37}$$

Obviously, the loop corrections to equation (36) contain IR singularities. This singularities can be taken into account using RG method. This procedure leads to the fact that charges g_{0j},λ_{0j} in (36) must now be replaced by the invariant charges $\bar{g}_j,\bar{\lambda}_j$, which in turn depend on the parameter τ. After such processing, the contributions of higher loops give only ε-corrections to the mean field theory results. Let us introduce $z_j\equiv\beta_j/M^{d_\beta}, s\equiv\tau/M^2$, where $d_\beta=1-\varepsilon/2$ is canonical dimension of the field β. Then the RG equations for the invariant variables are

$$\partial_\xi\bar{g}_j=\frac{\beta_{g_j}}{2+\gamma_\tau},\quad \bar{g}_j\big|_{\xi=0}=g_j, \tag{38}$$

$$\partial_\xi\bar{\lambda}_j=\frac{\beta_{\lambda_j}}{2+\gamma_\tau},\quad \bar{\lambda}_j\big|_{\xi=0}=\lambda_j, \tag{39}$$

$$\partial_\xi\bar{z}_j=-\bar{z}_j\frac{\Delta_\beta+\gamma_\beta}{2+\gamma_\tau},\quad \bar{z}_j\big|_{\xi=0}=z_j. \tag{40}$$

Finally, if we combine previous equations with conditions (36) and (37), we get

$$|\bar{z}_j|^2=-\frac{9}{2}\frac{2n\bar{g}_1+\bar{g}_2}{4n^2\bar{\lambda}_1+2n\bar{\lambda}_2+\bar{\lambda}_3}, \tag{41}$$

$$\tau=\frac{9}{16}\frac{(2n\bar{g}_1+\bar{g}_2)^2}{4n^2\bar{\lambda}_1+2n\bar{\lambda}_2+\bar{\lambda}_3}, \tag{42}$$

n is the number of non-zero blocks. Thus, as τ decreases, the invariant charges intersect the boundary of the stability domain and new solution (41) of stationary equations (37) appears. This phase has two non-zero blocks, $n=2$. Equation (42) determines the transition temperature τ_t. In

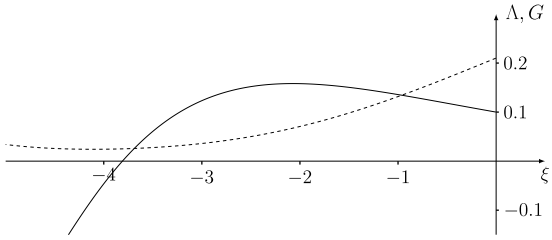

Fig. 6. Trajectories of "effective" coupling constants $\Lambda \equiv 4n^2\bar{\lambda}_1 + 2n\bar{\lambda}_2 + \bar{\lambda}_3$ (dashed line) and $G \equiv 2n\bar{g}_1 + \bar{g}_2$ (solid line) at $D = 3$ and $n = 2$.

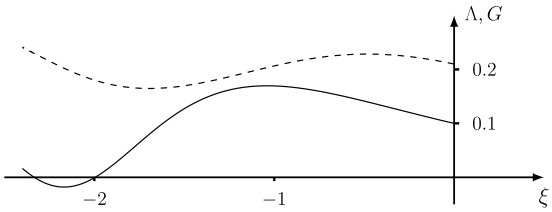

Fig. 7. Trajectories of "effective" coupling constants $\Lambda \equiv 4n^2\bar{\lambda}_1 + 2n\bar{\lambda}_2 + \bar{\lambda}_3$ (dashed line) and $G \equiv 2n\bar{g}_1 + \bar{g}_2$ (solid line) at $D = 2$ and $n = 2$.

order to solve equation (42) it is necessary to know solutions of RG equations (38) and (39). As before, the RG equations must be resummed. Similar to (15) we can rewrite the equations (39)

$$\partial_\xi \bar{\lambda}_i = -\frac{2\varepsilon - 2}{\varepsilon}\bar{\lambda}_i + \sum_{N=0}^{K} \varepsilon^N \bar{\lambda}_j L_{ji}^{(N)}(\bar{g}_1, \bar{g}_2),$$
$$\bar{\lambda}_i\big|_{\xi=0} = \lambda_i. \tag{43}$$

The HOA for $L_{ji}^{(N)}$ are needed for the Borel resummation too. Our analysis in Sect. 2 shows that calculation of $L_{ji}^{(N)}$ coefficients is connected with the renormalization of six-point 1PI Green functions ($\sim (\sqrt{N})^6$) which include one insertion of composite operators $F_j \sim (\sqrt{N})^6$, hence $L_{ji}^{(N)}/(\sqrt{N})^{6+6} \sim B_i^{(N)}/(\sqrt{N})^4$. Indices structure is irrelevant for the HOA.

Thus, we can resum the RG equations (43) by the formula (29). The results of numerical computations are shown in Figs. 6 and 7. This allows us to solve the equation (42). As a result, the root of this equation ξ_c differs only a little from ξ_0 obtained in Sect. 3. Remember that ξ_0 demonstrates a weak dependence from initial values of the coupling constants g_i.

Let us discus here the possible contributions of f operators (35) to the results obtained. There are some reasons why we have not calculated these counterterms.

First, we can state that these contributions are relatively small compared with F because f operators are more IR irrelevant in the real space dimensions $D = 2, 3$ then F according to the canonical dimensions mentioned above. Then the corresponding invariant charges will be oppressed by the first terms in the RG equations similar to (43) for these variables.

Second, it can be simply shown by the instanton analysis presented, that the high-order contributions of f operators are small in $1/N$ compared with these of F.

And third, the calculations of the renormalization of the full family of composite operators F and f is rather technically difficult now. To calculate the full renormalization constants matrix

up to ε^3 corrections one needs to consider six-loop diagrams. It is not worth while to start these calculations, as our results show that the first order phase transition takes place and the influence of F operators on it's temperature is rather small.

Taking all this into account we can state that in the model considered the first-order phase transition takes place at a temperature higher than the predictions for continuous phase transitions. To estimate the temperature difference in $D = 3$ case we have calculated numerically that $\zeta_0 = \tau_t / g_2^2 \approx 2 \div 3$ in a wide range of values $g_2 \approx 10^{-5} \div 0.1$, here τ_t is the root of the equation (42). It is natural to assume that the charges are of the same order of magnitude $g_1 \sim g_2 << 1$. Then the renormalization constants Z_d have the form $Z_d = 1 + O(g_j)$. In this approximation the ratio $Z_\tau / Z_{g_2}^2$ equals to 1. This leads to the relation

$$\tau_0 / g_{02}^2 = \zeta_0. \tag{44}$$

The integrals over momenta and the sum over frequencies ω_s (7), (8) can be reduced to the one-dimensional integrals. But the RG-approach used in our article gives us an opportunity to calculate different values for small τ only. Thus, it is sufficient to calculate these parameters (7), (8) using the approximation $\beta\delta >> 1$. It can be found in this approximation

$$\widetilde{g}_{02} \approx \frac{7 v_F \beta}{8(\pi T)^2} \zeta(3), \quad \widetilde{\tau}_0 \approx \frac{\beta}{2\lambda} \left(1 - \lambda v_F \ln \frac{\gamma \delta}{\pi T} \right), \quad c_0 \approx \frac{7 v_F p_F^2 \beta}{96(\pi T m)^2} \zeta(3), \tag{45}$$

with corrections $\sim O((\beta\delta)^{-1})$. Here $v_F = m p_F / (2\pi^2)$ is $3D$-density of states at the Fermi level, p_F is the Fermi momentum. Near the transition point τ_0 can be estimated as

$$\tau_0 \approx \frac{\beta v_F}{2 c_0} \frac{\Delta T}{T_0}, \tag{46}$$

where T_0 is the continuous phase transition temperature determined by the usual approach [1]. Combining (44), (45), (46) we get the estimation for the temperature difference between the first order phase transition and T_0

$$\frac{\Delta T}{T_0} = \zeta_0 \frac{6912 \pi^6}{7 \zeta(3)} \left(\frac{T_0}{T_F} \right)^4. \tag{47}$$

5. Conclusions

In contrast to the case of the electron systems ($r = 2$, r – number of spin degrees of freedom) where continuous phase transition takes place, our investigation has shown that in systems with high spin fermions ($r \geq 4$) critical fluctuations destroy stability of the system (see Fig. 2). In such systems the first order phase transitions take place in space dimension $D = 3$. These results were obtained by means of renormalization group analysis with ε-expansion up to the fifth-loop order of perturbation theory and subsequent Borel resummation. It should be noted that five loop calculations are indispensable to be sure that the first order phase transition takes place.

The temperature of the transition to the superconducting or the superfluid phase was estimated for the systems under consideration. Three loop RG analysis for composite operators, which are similar to $(\chi \chi^\dagger)^3$ in the Landau–Ginzburg functional, was performed for estimation of this temperature. It was revealed that the transition temperature is higher than the theoretical estimation based on the continuous phase transition formalism for the same model. The obtained difference in temperatures is rather small (see expr. (47)). But it should be kept in mind that the approach

used in the present work is applicable for the small deviations from the phase transition temperature only. Thus, in any case, we can guarantee that the difference in the phase transition temperature is not lower than our estimation.

As for $2D$ systems, one can state that the five loop approximation is not sufficient to determine neither the phase transition type nor the phase transition temperature. The last is an excellent example in favor of further development of the high-loop calculations.

Acknowledgements

G.A. Kalagov and M.Yu. Nalimov are grateful to SPbSU Grant 11.38.636.2013, M.V. Kompaniets is supported by SPbSU Grant 11.38.185.2014.

Appendix A

The five-loop results for the β_{g_i}, four-loop results for the anomalous dimension γ_τ and three-loop approximations for β_{λ_i} are presented here.

$$
\begin{aligned}
\gamma_\tau = &-\frac{1}{4}(r^2-r+2)g_1 - \frac{1}{2}(r-1)g_2 + \frac{5}{32}(r^2-r+2)g_1^2 \\
&+ \frac{5}{8}(r-1)g_1g_2 + \frac{5}{64}(r^2-3r+4)g_2^2 \\
&- \frac{1}{256}(15r^4-30r^3+156r^2-141r+222)g_1^3 \\
&- \frac{3}{128}(15r^3-30r^2+126r-111)g_1^2g_2 \\
&- \frac{3}{1024}(r^4-4r^3+403r^2-960r+888)g_1g_2^2 \\
&- \frac{1}{1024}(90r^3-321r^2+987r-888)g_2^3 + \frac{{g_1}^4}{122\,880}\Big[(720\,\zeta\,(3)-5)\,r^6 \\
&+ (-2160\,\zeta\,(3)+15)\,r^5 + \Big(80\,\pi^4+6000\,\zeta\,(3)+37\,865\Big)\,r^4 \\
&+ \Big(-160\,\pi^4-8400\,\zeta\,(3)-75\,755\Big)\,r^3 + \Big(592\,\pi^4+24\,960\,\zeta\,(3)+268\,960\Big)\,r^2 \\
&+ \Big(-512\,\pi^4-21\,120\,\zeta\,(3)-231\,080\Big)\,r + 704\,\pi^4+32\,640\,\zeta\,(3)+310\,600\Big] \\
&+ \frac{g_2{g_1}^3}{15\,360}\Big[(720\,\zeta\,(3)-5)\,r^5 \\
&+ (-2160\,\zeta\,(3)+15)\,r^4 + \Big(80\,\pi^4+4560\,\zeta\,(3)+37\,875\Big)\,r^3 \\
&+ \Big(-160\,\pi^4-5520\,\zeta\,(3)-75\,775\Big)\,r^2 + \Big(432\,\pi^4+18\,720\,\zeta\,(3)+193\,190\Big)\,r \\
&- 352\,\pi^4-16\,320\,\zeta\,(3)-155\,300\Big] \\
&+ \frac{{g_2}^2{g_1}^2}{30\,720}\Big[\Big(12\,\pi^4+3240\,\zeta\,(3)+6885\Big)\,r^4 + \Big(-48\,\pi^4-8640\,\zeta\,(3)-27\,570\Big)\,r^3
\end{aligned}
$$

$$
\begin{aligned}
&+\left(636\pi^4+28\,440\zeta(3)+293\,850\right)r^2\\
&+\left(-1320\pi^4-54\,720\zeta(3)-592\,155\right)r+1056\pi^4+48\,960\zeta(3)+465\,900\Big]\\
&+\frac{g_1{g_2}^3}{30\,720}\Big[(-120\zeta(3)+250)r^5+(780\zeta(3)-1625)r^4\\
&+\left(80\pi^4+3960\zeta(3)+40\,620\right)r^3\\
&+\left(-368\pi^4-19\,380\zeta(3)-170\,520\right)r^2+\left(896\pi^4+40\,920\zeta(3)+400\,625\right)r\\
&-704\pi^4-32\,640\zeta(3)-310\,600\Big]\\
&+\frac{{g_2}^4}{245\,760}\Big[\left(16\pi^4+480\zeta(3)+7505\right)r^4+\left(-144\pi^4-4320\zeta(3)-67\,910\right)r^3\\
&+\left(800\pi^4+36\,240\zeta(3)+370\,210\right)r^2\\
&+\left(-1728\pi^4-85\,680\zeta(3)-781\,655\right)r+1408\pi^4+65\,280\zeta(3)+621\,200\Big]
\end{aligned}
\tag{48}
$$

$$
\begin{aligned}
\beta_{g_1}=&-\varepsilon g_1+\frac{g_1^2}{4}(r^2-r+8)+(r-1)g_1g_2+\frac{3}{4}g_2^2\\
&-\frac{9}{48}(3r^2-3r+14)g_1^3-\frac{11}{4}(r-1)g_1^2g_2-\frac{g_1g_2^2}{32}(5r^2-15r+92)-\frac{3}{8}(r-2)g_2^3\\
&+\frac{g_1^4}{512}\Big[33r^4-66r^3+(955+480\zeta(3))r^2-(480\zeta(3)+922)r+2960\\
&+2112\zeta(3)\Big]+\frac{g_1^3g_2}{128}\Big[79r^3-158r^2+(1397+768\zeta(3))r-1318-768\zeta(3)\Big]\\
&+\frac{g_1^2g_2^2}{1024}\Big[3r^4-12r^3+(576\zeta(3)+3355)r^2-(1728\zeta(3)+7568)r+9216\zeta(3)\\
&+14\,788\Big]+\frac{g_1g_2^3}{512}\Big[60r^3-321r^2+(2943+1152\zeta(3))r-2304\zeta(3)-4092\Big]\\
&+\frac{g_2^4}{1024}\Big[(96\zeta(3)+193)r^2-(576\zeta(3)+891)r+1536\zeta(3)+1860\Big]\\
&+\frac{{g_1}^2{g_2}^3}{30\,720}\Big[(120\zeta(3)-250)r^5+(-780\zeta(3)+1625)r^4\\
&+\left(-16\pi^4-48\,840\zeta(3)-19\,200\zeta(5)-77\,850\right)r^3\\
&+(\,136\pi^4+189\,900\zeta(3)+105\,600\zeta(5)+362\,465\,)r^2\\
&+\left(1880\pi^4-1\,291\,440\zeta(3)-1\,747\,200\zeta(5)-1\,650\,130\right)r\\
&-3488\pi^4+1\,822\,080\zeta(3)+2\,726\,400\zeta(5)+1\,863\,040\Big]
\end{aligned}
$$

$$
\begin{aligned}
&+\frac{{g_1}^4 g_2}{3840}\Big[(-90\,\zeta\,(3)+70)\,r^5+(270\,\zeta\,(3)-210)\,r^4\\
&+\Big(38\,\pi^4-16\,830\,\zeta\,(3)-12\,000\,\zeta\,(5)-19\,575\Big)\,r^3\\
&+\Big(-76\,\pi^4+33\,210\,\zeta\,(3)+24\,000\,\zeta\,(5)+39\,500\Big)\,r^2+\Big(378\,\pi^4-162\,240\,\zeta\,(3)\\
&-242\,400\,\zeta\,(5)-179\,455\Big)\,r-340\,\pi^4+145\,680\,\zeta\,(3)+230\,400\,\zeta\,(5)+159\,670\Big]\\
&+\frac{{g_1}^3 {g_2}^2}{15\,360}\Big[(-5040\,\zeta\,(3)-2025)\,r^4+(16\,920\,\zeta\,(3)+10\,560)\,r^3\\
&+\Big(472\,\pi^4-288\,720\,\zeta\,(3)-304\,800\,\zeta\,(5)-405\,490\Big)\,r^2\\
&+\Big(-920\,\pi^4+583\,560\,\zeta\,(3)+703\,200\,\zeta\,(5)+861\,425\Big)\,r+2320\,\pi^4\\
&-1\,111\,680\,\zeta\,(3)-1\,708\,800\,\zeta\,(5)-1\,122\,820\Big]\\
&+\frac{g_1 {g_2}^4}{122\,880}\Big[\Big(-16\,\pi^4-480\,\zeta\,(3)-7505\Big)\,r^4+\Big(144\,\pi^4+4320\,\zeta\,(3)+67\,910\Big)\,r^3\\
&+\Big(544\,\pi^4-555\,120\,\zeta\,(3)-556\,800\zeta(5)-763\,450\Big)\,r^2\\
&+\Big(-3744\pi^4+2\,224\,080\zeta(3)+2\,678\,400\zeta(5)+2\,397\,215\Big)\,r\\
&+7424\pi^4-3\,820\,800\zeta(3)-5\,875\,200\zeta(5)-3\,293\,840\Big]\\
&+\frac{{g_1}^5}{61\,440}\Big[25\,r^6-75\,r^5+\Big(80\,\pi^4-30\,240\,\zeta\,(3)-19\,200\,\zeta\,(5)-31\,525\Big)\,r^4\\
&+\Big(-160\,\pi^4+60\,480\,\zeta\,(3)+38\,400\,\zeta\,(5)+63\,175\Big)\,r^3\\
&+\Big(1072\,\pi^4-396\,960\,\zeta\,(3)-547\,200\,\zeta\,(5)-433\,880\Big)\,r^2\\
&+\Big(-992\,\pi^4+366\,720\,\zeta\,(3)+528\,000\,\zeta\,(5)+402\,280\Big)\,r+2816\,\pi^4\\
&-1\,119\,360\,\zeta\,(3)-1\,785\,600\,\zeta\,(5)-983\,240\Big]\\
&+\frac{{g_2}^5}{30\,720}\Big[\Big(8\,\pi^4-1800\,\zeta\,(5)-3000\,\zeta\,(3)-1940\Big)\,r^3\\
&+\Big(-68\,\pi^4+22\,800\,\zeta\,(5)+26\,100\,\zeta\,(3)+19\,745\Big)\,r^2\\
&+\Big(320\,\pi^4-162\,600\,\zeta\,(5)-127\,140\,\zeta\,(3)-105\,495\Big)\,r-464\,\pi^4\\
&+294\,000\,\zeta\,(5)+187\,440\,\zeta\,(3)+150\,480\Big]\\
&+\frac{{g_2}^6}{165\,150\,720}\Big[\Big(-4000\,\pi^6-62\,832\,\pi^4-423\,360\,(\zeta\,(3))^2+11\,914\,560\,\zeta\,(5)
\end{aligned}
$$

$$
\begin{aligned}
&+ 11\,113\,200\,\zeta\,(7) + 9\,969\,120\,\zeta\,(3) + 2\,082\,360\Big) r^4 \\
&+ \Big(64\,800\,\pi^6 + 706\,608\,\pi^4 + 2\,721\,600\,(\zeta\,(3))^2 - 188\,798\,400\,\zeta\,(5) \\
&- 182\,256\,480\,\zeta\,(7) - 124\,699\,680\,\zeta\,(3) - 66\,122\,280\Big) r^3 \\
&- \Big(669\,600\,\pi^6 + 4\,704\,000\,\pi^4 - 3\,205\,440\zeta\,(3)^2 - 1\,928\,928\,960\zeta\,(5) \\
&- 1\,953\,700\,560\zeta(7) + 1\,036\,934\,640\zeta(3) + 685\,670\,475\Big) r^2 \\
&+ \Big(2\,359\,200\,\pi^6 + 13\,216\,896\,\pi^4 - 207\,023\,040\,(\zeta\,(3))^2 - 6\,794\,303\,040\,\zeta\,(5) \\
&- 7\,890\,372\,000\,\zeta\,(7) - 3\,424\,896\,720\,\zeta\,(3) \\
&- 2\,185\,479\,765\Big) r - 3\,105\,600\,\pi^6 - 14\,812\,896\,\pi^4 + 582\,906\,240\zeta\,(3)^2 \\
&+ 8\,967\,934\,080\zeta\,(5) + 12\,429\,002\,880\zeta\,(7) + 4\,364\,680\,320\zeta\,(3) + 2\,542\,700\,160\Big] \\
&+ \frac{{g_1}^6}{82\,575\,360}\Big[(-45\,360\,\zeta\,(3) + 4095)\, r^8 + (181\,440\,\zeta\,(3) - 16\,380)\, r^7 \\
&+ \Big(-6400\,\pi^6 - 63\,504\,\pi^4 - 1\,451\,520\,(\zeta\,(3))^2 + 24\,595\,200\,\zeta\,(5) \\
&+ 6\,017\,760\,\zeta\,(3) + 3\,986\,640\Big) r^6 \\
&+ \Big(19\,200\,\pi^6 + 190\,512\,\pi^4 + 4\,354\,560\,(\zeta\,(3))^2 - 73\,785\,600\,\zeta\,(5) \\
&- 18\,688\,320\,\zeta\,(3) - 11\,902\,590\Big) r^5 \\
&+ \Big(-246\,400\,\pi^6 - 1\,589\,616\,\pi^4 - 18\,627\,840\,(\zeta\,(3))^2 + 675\,843\,840\,\zeta\,(5) \\
&+ 497\,871\,360\,\zeta\,(7) + 359\,730\,000\,\zeta\,(3) + 266\,566\,545\Big) r^4 \\
&+ \Big(460\,800\,\pi^6 + 2\,861\,712\,\pi^4 + 29\,998\,080\,(\zeta\,(3))^2 - 1\,228\,711\,680\,\zeta\,(5) \\
&- 995\,742\,720\,\zeta\,(7) - 688\,101\,120\,\zeta\,(3) - 513\,314\,550\Big) r^3 \\
&+ \Big(-2\,230\,400\,\pi^6 - 11\,007\,360\,\pi^4 + 93\,623\,040\,(\zeta\,(3))^2 + 6\,003\,809\,280\,\zeta\,(5) \\
&+ 7\,219\,134\,720\,\zeta\,(7) + 3\,124\,396\,800\,\zeta\,(3) + 2\,348\,272\,080\Big) r^2 \\
&+ \Big(2\,003\,200\,\pi^6 + 9\,608\,256\,\pi^4 - 107\,896\,320\,(\zeta\,(3))^2 - 5\,401\,751\,040\,\zeta\,(5)\,. \\
&- 6\,721\,263\,360\,\zeta\,(7) - 2\,783\,491\,200\,\zeta\,(3) - 2\,093\,595\,840\Big) r \\
&- 4\,761\,600\,\pi^6 - 21\,288\,960\,\pi^4 + 789\,626\,880\,(\zeta\,(3))^2 + 13\,312\,373\,760\,\zeta\,(5) \\
&+ 18\,705\,738\,240\,\zeta\,(7) + 6\,624\,253\,440\,\zeta\,(3) + 4\,150\,863\,360\Big] \\
&+ \frac{{g_1}^3 {g_2}^3}{61\,931\,520}\Big[(\,-148\,176\pi^4 + 20\,684\,160\zeta\,(5) + 26\,308\,800\zeta\,(3) + 9\,035\,460\,)\, r^5
\end{aligned}
$$

$$
\begin{aligned}
&+ (\, 600\,264\,\pi^4 - 115\,577\,280\,\zeta\,(5) - 126\,675\,360\,\zeta\,(3) - 63\,253\,575\,) \, r^4 \\
&+ (\, -1\,040\,000\,\pi^6 - 8\,538\,768\,\pi^4 - 218\,937\,600\,\left(\zeta\,(3)\right)^2 + 4\,642\,807\,680\,\zeta\,(5) \\
&+ 2\,453\,794\,560\,\zeta\,(7) + 2\,527\,701\,120\,\zeta\,(3) + 2\,508\,172\,380\,) \, r^3 \\
&+ (\, 2\,996\,800\,\pi^6 + 23\,098\,824\,\pi^4 + 647\,982\,720\,\left(\zeta\,(3)\right)^2 \\
&- 15\,032\,969\,280\,\zeta\,(5) - 10\,775\,358\,720\,\zeta\,(7) - 8\,813\,327\,040\,\zeta\,(3) \\
&- 9\,558\,318\,105\,) \, r^2 + (\, -15\,726\,400\,\pi^6 - 81\,409\,104\,\pi^4 \\
&+ 1\,124\,323\,200\,\left(\zeta\,(3)\right)^2 + 56\,995\,142\,400\,\zeta\,(5) + 70\,626\,608\,640\,\zeta\,(7) \\
&+ 32\,122\,349\,280\,\zeta\,(3) + 27\,417\,665\,520\,) \, r + 20\,652\,800\,\pi^6 \\
&+ 96\,473\,664\,\pi^4 - 3\,306\,078\,720\,\left(\zeta\,(3)\right)^2 - 66\,934\,425\,600\,\zeta\,(5) \\
&- 92\,710\,759\,680\,\zeta\,(7) - 36\,282\,556\,800\,\zeta\,(3) - 25\,755\,125\,760 \Big] \\
&+ \frac{{g_1}^2 {g_2}^4}{495\,452\,160} \Big[\Big(11\,088\,\pi^4 - 1\,118\,880\,\zeta\,(3) - 967\,680\,\zeta\,(5) + 2\,237\,760 \Big) \, r^6 \\
&+ (\, -94\,752\,\pi^4 + 11\,370\,240\,\zeta\,(3) + 9\,676\,800\,\zeta\,(5) \\
&- 24\,388\,560\,) \, r^5 + (\, 57\,600\,\pi^6 - 2\,762\,928\,\pi^4 - 82\,736\,640\,\left(\zeta\,(3)\right)^2 \\
&+ 1\,043\,506\,800\,\zeta\,(3) + 1\,074\,124\,800\,\zeta\,(5) \\
&+ 320\,060\,160\,\zeta\,(7) + 999\,549\,495\,) \, r^4 + (\, -784\,000\,\pi^6 + 10\,469\,088\,\pi^4 \\
&+ 650\,039\,040\,\left(\zeta\,(3)\right)^2 - 6\,436\,765\,440\,\zeta\,(3) \\
&- 6\,812\,467\,200\,\zeta\,(5) - 2\,880\,541\,440\,\zeta\,(7) - 7\,398\,362\,160\,) \, r^3 \\
&+ (\, -21\,820\,800\,\pi^6 - 144\,452\,448\,\pi^4 - 2\,378\,315\,520\,\left(\zeta\,(3)\right)^2 \\
&+ 56\,439\,013\,680\,\zeta\,(3) + 95\,710\,325\,760\,\zeta\,(5) + 88\,816\,694\,400\,\zeta\,(7) \\
&+ 53\,612\,539\,785\,) \, r^2 + (\, 81\,120\,000\,\pi^6 + 444\,237\,696\,\pi^4 \\
&- 3\,540\,257\,280\,\left(\zeta\,(3)\right)^2 - 163\,022\,146\,560\,\zeta\,(3) - 290\,900\,574\,720\,\zeta\,(5) \\
&- 334\,622\,897\,280\,\zeta\,(7) - 131\,226\,822\,720\,) \, r - 122\,828\,800\,\pi^6 - 576\,559\,872\,\pi^4 \\
&+ 23\,835\,893\,760\,\left(\zeta\,(3)\right)^2 + 208\,349\,245\,440\,\zeta\,(3) + 400\,734\,673\,920\,\zeta\,(5) \\
&+ 557\,544\,798\,720\,\zeta\,(7) + 136\,273\,132\,800 \Big] \\
&+ \frac{g_1 {g_2}^5}{123\,863\,040} \Big[\Big(1600\,\pi^6 + 11\,088\,\pi^4 - 120\,960\,\left(\zeta\,(3)\right)^2 - 120\,960\,\zeta\,(5) \\
&+ 1\,481\,760\zeta\,(3) + 2\,419\,200 \Big) r^5 + \Big(-23\,200\pi^6 - 127\,008\pi^4 + 2\,842\,560\,\left(\zeta\,(3)\right)^2 \\
&+ 483\,840\,\zeta\,(5) - 15\,558\,480\,\zeta\,(3) - 45\,412\,920 \Big) r^4 \\
&+ (\, -176\,800\,\pi^6 - 2\,054\,304\,\pi^4 - 48\,686\,400\,\left(\zeta\,(3)\right)^2 + 1\,077\,148\,800\,\zeta\,(5) \\
&+ 750\,632\,400\,\zeta\,(3) + 840\,157\,920\,\zeta\,(7) \\
&+ 696\,512\,565\,) \, r^3 + (\, 1\,904\,000\,\pi^6 + 14\,635\,656\,\pi^4 + 93\,381\,120\,\left(\zeta\,(3)\right)^2 \\
&- 7\,451\,619\,840\zeta\,(5) - 4\,707\,944\,640\zeta\,(3) - 7\,201\,353\,600\zeta\,(7) - 3\,622\,361\,715\,) \, r^2
\end{aligned}
$$

$$
\begin{aligned}
&+ (-9\,401\,600\,\pi^6 - 51\,609\,096\,\pi^4 + 656\,328\,960\ (\zeta\ (3))^2 + 30\,318\,503\,040\,\zeta\ (5) \\
&+ 16\,431\,750\,720\,\zeta\ (3) + 35\,966\,760\,480\,\zeta\ (7) + 11\,409\,189\,120\ )\, r \\
&+ 12\,768\,000\,\pi^6 + 60\,399\,360\,\pi^4 - 2\,223\,728\,640\ (\zeta\ (3))^2 - 39\,762\,938\,880\,\zeta\ (5) \\
&- 19\,683\,699\,840\,\zeta\ (3) - 54\,170\,182\,080\,\zeta\ (7) - 12\,379\,268\,160\Big] \\
&+ \frac{{g_1}^5 g_2}{20\,643\,840}\Big[\Big(-1008\,\pi^4 - 85\,680\,\zeta\ (3) + 50\,715\Big)\, r^7 \\
&+ \Big(4032\,\pi^4 + 342\,720\,\zeta\ (3) - 202\,860\Big)\, r^6 \\
&+ \Big(-19\,200\,\pi^6 - 178\,416\,\pi^4 - 4\,354\,560\ (\zeta\ (3))^2 + 20\,049\,120\,\zeta\ (3) \\
&+ 72\,817\,920\,\zeta\ (5) + 12\,836\,040\Big) r^5 \\
&+ \Big(57\,600\,\pi^6 + 521\,136\,\pi^4 + 13\,063\,680\ (\zeta\ (3))^2 - 61\,346\,880\,\zeta\ (3) \\
&- 218\,453\,760\,\zeta\ (5) - 37\,798\,110\Big) r^4 + (-579\,200\,\pi^6 - 3\,661\,728\,\pi^4 \\
&- 36\,046\,080\ (\zeta\ (3))^2 + 1\,386\,927\,360\zeta\ (7) + 930\,903\,120\zeta\ (3) + 1\,686\,666\,240\zeta\ (5) \\
&+ 729\,900\,045\ )\, r^3 + (1\,062\,400\,\pi^6 + 6\,459\,600\,\pi^4 + 50\,319\,360\ (\zeta\ (3))^2 \\
&- 2\,773\,854\,720\zeta\ (7) - 1\,759\,161\,600\zeta\ (3) - 3\,009\,242\,880\zeta\ (5) - 1\,397\,039\,910\ )\, r^2 \\
&+ (-3\,600\,000\,\pi^6 - 16\,821\,504\,\pi^4 + 357\,799\,680\ (\zeta\ (3))^2 + 13\,975\,960\,320\,\zeta\ (7) \\
&+ 5\,577\,022\,080\,\zeta\ (3) + 10\,568\,759\,040\,\zeta\ (5) + 4\,303\,830\,720\ )\, r + 3\,078\,400\,\pi^6 \\
&+ 13\,677\,888\,\pi^4 - 380\,782\,080\ (\zeta\ (3))^2 \\
&- 12\,589\,032\,960\zeta\ (7) - 4\,707\,722\,880\zeta\ (3) - 9\,100\,546\,560\zeta\ (5) - 3\,611\,576\,640\Big] \\
&+ \frac{{g_1}^4 {g_2}^2}{82\,575\,360}\Big[\Big(-43\,344\,\pi^4 + 1\,814\,400\,\zeta\ (5) + 3\,412\,080\,\zeta\ (3) + 579\,915\Big)\, r^6 \\
&+ (172\,368\,\pi^4 - 9\,072\,000\,\zeta\ (5) - 17\,735\,760\,\zeta\ (3) \\
&- 833\,805\ )\, r^5 + (-432\,000\,\pi^6 - 3\,820\,992\,\pi^4 - 83\,946\,240\ (\zeta\ (3))^2 \\
&+ 1\,664\,167\,680\,\zeta\ (5) + 671\,968\,080\,\zeta\ (3) + 266\,716\,800\,\zeta\ (7) + 508\,858\,035\ )\, r^4 \\
&+ (1\,318\,400\,\pi^6 + 11\,238\,864\,\pi^4 + 242\,887\,680\ (\zeta\ (3))^2 - 5\,122\,051\,200\,\zeta\ (5) \\
&- 2\,143\,839\,600\,\zeta\ (3) - 1\,066\,867\,200\,\zeta\ (7) - 1\,768\,425\,435\ )\, r^3 \\
&+ (-9\,465\,600\,\pi^6 - 55\,073\,424\,\pi^4 - 194\,019\,840\ (\zeta\ (3))^2 \\
&+ 31\,538\,989\,440\,\zeta\ (5) + 17\,855\,752\,320\,\zeta\ (3) + 32\,539\,449\,600\,\zeta\ (7) \\
&+ 15\,773\,492\,490\ )\, r^2 + (16\,310\,400\,\pi^6 + 85\,935\,360\,\pi^4 \\
&- 319\,092\,480\ (\zeta\ (3))^2 - 55\,724\,820\,480\,\zeta\ (5) - 32\,871\,968\,640\,\zeta\ (3) \\
&- 67\,479\,350\,400\,\zeta\ (7) - 30\,066\,795\,360\ )\, r - 25\,849\,600\,\pi^6 - 117\,273\,408\,\pi^4 \\
&+ 4\,275\,694\,080\ (\zeta\ (3))^2 + 80\,392\,435\,200\,\zeta\ (5) + 42\,975\,515\,520\,\zeta\ (3) \\
&+ 113\,087\,923\,200\,\zeta\ (7) + 30\,838\,536\,960\Big] \qquad (49)
\end{aligned}
$$

$$
\begin{aligned}
\beta_{g_2} = &-\varepsilon g_2 + \frac{1}{4}(2r-5)g_2^2 + 3g_1g_2 - \frac{3}{32}(r^2-7r+20)g_2^3 \\
&- \frac{1}{4}(11r-20)g_2^2g_1 - \frac{1}{16}(5r^2-5r+82)g_1^2g_2 \\
&+ \frac{g_2^4}{1024}\left[26r^3 - (383+96\zeta(3))r^2 + (2459+1152\zeta(3))r - 4060 - 2688\zeta(3)\right] \\
&+ \frac{g_2^3g_1}{128}\left[(96\zeta(3)+182)r^2 - (963+576\zeta(3))r + 1536\zeta(3) + 1937\right] \\
&+ \frac{g_1^2g_2^2}{512}\left[-70r^3 + 11r^2 + (6423+4608\zeta(3))r - 8064\zeta(3) - 10\,366\right] \\
&+ \frac{g_1^3g_2}{256}\Big[-13r^4 + 26r^3 + (192\zeta(3)+355)r^2 - (368+192\zeta(3))r \\
&+ 3284 + 2688\zeta(3)\Big] + \frac{{g_2}^6}{165\,150\,720}\Big[\Big(-800\pi^6 + 2016\pi^4 - 181\,440\,(\zeta(3))^2 \\
&+ 3\,124\,800\,\zeta(5) - 1\,229\,760\,\zeta(3) + 274\,680\Big)r^5 + \Big(14\,800\pi^6 + 17\,136\pi^4 \\
&+ 5\,473\,440\,(\zeta(3))^2 - 46\,478\,880\,\zeta(5) + 7\,207\,200\,\zeta(3) - 17\,781\,120\,\zeta(7) \\
&- 18\,961\,740\Big)r^4 + \Big(-216\,800\pi^6 - 971\,376\pi^4 - 40\,944\,960\,(\zeta(3))^2 \\
&+ 548\,694\,720\,\zeta(5) + 211\,095\,360\,\zeta(3) + 444\,528\,000\,\zeta(7) + 310\,764\,930\Big)r^3 \\
&+ (\,1\,487\,600\pi^6 + 7\,296\,576\pi^4 + 106\,656\,480\,(\zeta(3))^2 - 3\,759\,850\,080\,\zeta(5) \\
&- 2\,000\,360\,880\,\zeta(3) - 3\,876\,284\,160\,\zeta(7) - 1\,849\,193\,115\,)\,r^2 + (\,-5\,115\,200\pi^6 \\
&- 23\,668\,512\pi^4 + 240\,347\,520\,(\zeta(3))^2 + 13\,534\,899\,840\zeta(5) + 7\,160\,877\,360\zeta(3) \\
&+ 16\,491\,988\,800\,\zeta(7) + 5\,356\,768\,095\,)\,r + 6\,417\,600\pi^6 + 27\,765\,024\pi^4 \\
&- 996\,347\,520\,(\zeta(3))^2 - 17\,656\,813\,440\,\zeta(5) \\
&- 8\,883\,826\,560\,\zeta(3) - 24\,982\,473\,600\,\zeta(7) - 5\,759\,026\,560\Big] \\
&+ \frac{g_2{g_1}^5}{20\,643\,840}\Big[\Big(504\pi^4 - 25\,200\,\zeta(3) - 19\,215\Big)r^8 \\
&+ \Big(-2016\pi^4 + 100\,800\,\zeta(3) + 76\,860\Big)r^7 \\
&+ \Big(-5040\pi^4 + 483\,840\,\zeta(5) - 912\,240\,\zeta(3) - 488\,775\Big)r^6 \\
&+ \Big(22\,176\pi^4 - 1\,451\,520\,\zeta(5) + 2\,383\,920\,\zeta(3) + 1\,197\,315\Big)r^5 \\
&+ \Big(-60\,800\pi^6 - 378\,168\pi^4 - 5\,564\,160\,(\zeta(3))^2 + 97\,614\,720\,\zeta(5) \\
&+ 53\,837\,280\,\zeta(3) + 53\,343\,360\,\zeta(7) + 22\,215\,900\Big)r^4 \\
&+ \Big(121\,600\pi^6 + 717\,024\pi^4 + 11\,128\,320\,(\zeta(3))^2 - 192\,810\,240\,\zeta(5) \\
&- 111\,530\,160\,\zeta(3) - 106\,686\,720\,\zeta(7) - 46\,337\,655\Big)r^3
\end{aligned}
$$

$$
\begin{aligned}
&+ (-1\,004\,800\,\pi^6 - 4\,784\,304\,\pi^4 - 11\,128\,320\ (\zeta\,(3))^2 + 2\,180\,304\,000\,\zeta\,(5) \\
&+ 1\,008\,221\,760\,\zeta\,(3) + 2\,453\,794\,560\,\zeta\,(7) \\
&+ 665\,706\,930\ )\,r^2 + (\ 944\,000\,\pi^6 + 4\,429\,824\,\pi^4 + 5\,564\,160\ (\zeta\,(3))^2 \\
&- 2\,084\,140\,800\,\zeta\,(5) - 952\,076\,160\,\zeta\,(3) \\
&- 2\,400\,451\,200\,\zeta\,(7) - 642\,351\,360\ )\,r - 4\,064\,000\,\pi^6 - 18\,255\,552\,\pi^4 \\
&+ 803\,658\,240\ (\zeta\,(3))^2 + 10\,868\,014\,080\,\zeta\,(5) \\
&+ 5\,228\,657\,280\,\zeta\,(3) + 15\,469\,574\,400\,\zeta\,(7) + 2\,614\,718\,400\Big] \\
&+ \frac{{g_2}^2 {g_1}^4}{82\,575\,360}\Big[\Big(16\,128\,\pi^4 - 977\,760\,\zeta\,(3) - 485\,730\Big)\,r^7 \\
&+ \Big(-58\,464\,\pi^4 + 3\,865\,680\,\zeta\,(3) + 1\,518\,615\Big)\,r^6 \\
&+ (-25\,600\,\pi^6 - 374\,976\,\pi^4 - 5\,806\,080\ (\zeta\,(3))^2 + 71\,608\,320\,\zeta\,(5) \\
&- 20\,568\,240\,\zeta\,(3) - 18\,900\,525\ )\,r^5 + (\ 115\,200\,\pi^6 \\
&+ 1\,523\,088\,\pi^4 + 26\,127\,360\ (\zeta\,(3))^2 - 293\,207\,040\,\zeta\,(5) + 27\,362\,160\,\zeta\,(3) \\
&+ 53\,140\,815\ )\,r^4 + (-3\,398\,400\,\pi^6 - 19\,301\,856\,\pi^4 - 305\,303\,040\ (\zeta\,(3))^2 \\
&+ 5\,865\,592\,320\zeta\,(5) + 3\,119\,109\,840\zeta\,(3) + 4\,267\,468\,800\zeta\,(7) + 1\,522\,641\,015\ )\,r^3 \\
&+ (\ 8\,233\,600\,\pi^6 + 44\,209\,200\,\pi^4 + 731\,808\,000\ (\zeta\,(3))^2 \\
&- 14\,607\,855\,360\,\zeta\,(5) - 7\,731\,561\,600\,\zeta\,(3) - 11\,735\,539\,200\,\zeta\,(7) \\
&- 4\,037\,533\,710\ )\,r^2 + (-35\,196\,800\,\pi^6 - 158\,195\,520\,\pi^4 \\
&+ 3\,477\,116\,160\ (\zeta\,(3))^2 + 86\,228\,271\,360\,\zeta\,(5) + 40\,340\,401\,920\,\zeta\,(3) \\
&+ 114\,154\,790\,400\,\zeta\,(7) + 24\,959\,766\,720\ )\,r + 45\,574\,400\,\pi^6 + 202\,060\,992\,\pi^4 \\
&- 7\,568\,709\,120\ (\zeta\,(3))^2 - 119\,293\,171\,200\,\zeta\,(5) - 56\,388\,286\,080\,\zeta\,(3) \\
&- 167\,498\,150\,400\,\zeta\,(7) - 31\,424\,413\,440\Big] \\
&+ \frac{{g_2}^3 {g_1}^3}{30\,965\,760}\Big[\Big(16\,632\,\pi^4 + 423\,360\,\zeta\,(5) - 1\,988\,280\,\zeta\,(3) + 606\,060\Big)\,r^6 \\
&+ \Big(-42\,336\,\pi^4 - 3\,386\,880\,\zeta\,(5) + 7\,839\,720\,\zeta\,(3) - 3\,935\,295\Big)\,r^5 \\
&+ \Big(-150\,400\,\pi^6 - 1\,199\,016\,\pi^4 - 20\,563\,200\ (\zeta\,(3))^2 + 288\,368\,640\,\zeta\,(5) \\
&+ 73\,672\,200\,\zeta\,(3) + 53\,343\,360\,\zeta\,(7) - 7\,597\,170\Big)\,r^4 \\
&+ \Big(804\,800\,\pi^6 + 5\,532\,912\,\pi^4 + 124\,225\,920\ (\zeta\,(3))^2 - 1\,429\,989\,120\,\zeta\,(5) \\
&- 520\,377\,480\,\zeta\,(3) - 373\,403\,520\,\zeta\,(7) - 41\,148\,765\Big)\,r^3 \\
&+ (-7\,096\,000\,\pi^6 - 36\,004\,752\,\pi^4 - 120\,355\,200\ (\zeta\,(3))^2 + 14\,771\,695\,680\,\zeta\,(5) \\
&+ 7\,500\,170\,160\,\zeta\,(3) + 15\,656\,276\,160\,\zeta\,(7) + 4\,771\,718\,910\ )\,r^2 \\
&+ (\ 19\,315\,200\,\pi^6 + 90\,331\,920\,\pi^4 - 1\,239\,598\,080\ (\zeta\,(3))^2 - 45\,666\,270\,720\,\zeta\,(5)
\end{aligned}
$$

$$
\begin{aligned}
&- 22\,458\,915\,360\,\zeta(3) - 57\,744\,187\,200\,\zeta(7) - 14\,694\,406\,020\,)\,r \\
&- 25\,385\,600\,\pi^6 - 111\,430\,368\,\pi^4 + 4\,269\,162\,240\,(\zeta(3))^2 + 66\,375\,590\,400\,\zeta(5) \\
&+ 31\,540\,622\,400\,\zeta(3) + 93\,937\,656\,960\,\zeta(7) + 18\,253\,912\,320\Big] \\
&+ \frac{{g_2}^4 {g_1}^2}{123\,863\,040}\Big[\Big(-8000\,\pi^6 + 5040\,\pi^4 - 846\,720\,(\zeta(3))^2 + 20\,200\,320\,\zeta(5) \\
&- 10\,523\,520\,\zeta(3) - 2\,938\,950\Big) r^5 + \Big(100\,000\,\pi^6 + 702\,072\,\pi^4 \\
&+ 16\,027\,200\,(\zeta(3))^2 - 205\,873\,920\,\zeta(5) - 7\,968\,240\,\zeta(3) + 39\,434\,535\Big) r^4 \\
&+ (\,-3\,296\,800\,\pi^6 - 19\,813\,248\,\pi^4 - 248\,996\,160\,(\zeta(3))^2 \\
&+ 6\,816\,700\,800\zeta(5) + 3\,040\,752\,960\zeta(3) + 4\,880\,917\,440\zeta(7) + 2\,055\,979\,170\,)\,r^3 \\
&+ \Big(18\,913\,600\,\pi^6 + 98\,834\,904\,\pi^4 + 618\,226\,560\,(\zeta(3))^2 - 41\,966\,104\,320\,\zeta(5) \\
&- 19\,997\,757\,360\,\zeta(3) - 40\,967\,700\,480\,\zeta(7) - 14\,751\,336\,915\Big) r^2 \\
&+ (\,-63\,900\,800\,\pi^6 - 299\,922\,336\,\pi^4 + 4\,086\,270\,720\,(\zeta(3))^2 \\
&+ 154\,060\,583\,040\,\zeta(5) + 77\,286\,273\,120\,\zeta(3) + 194\,756\,607\,360\,\zeta(7) \\
&+ 52\,766\,403\,480\,)\,r + 76\,428\,800\,\pi^6 + 334\,861\,632\,\pi^4 \\
&- 11\,807\,631\,360\,(\zeta(3))^2 - 199\,344\,741\,120\,\zeta(5) - 96\,958\,391\,040\,\zeta(3) \\
&- 281\,492\,910\,720\,\zeta(7) - 59\,326\,142\,400\Big] \\
&+ \frac{{g_2}^5 g_1}{123\,863\,040}\Big[(\,-68\,800\,\pi^6 - 379\,008\,\pi^4 - 6\,773\,760\,(\zeta(3))^2 \\
&+ 161\,965\,440\,\zeta(5) + 51\,801\,120\,\zeta(3) + 100\,018\,800\,\zeta(7) + 76\,657\,770\,)\,r^4 \\
&+ (\,924\,800\,\pi^6 + 5\,057\,136\,\pi^4 + 99\,912\,960\,(\zeta(3))^2 - 2\,200\,383\,360\,\zeta(5) \\
&- 885\,336\,480\,\zeta(3) - 1\,760\,330\,880\,\zeta(7) - 1\,001\,516\,040\,)\,r^3 \\
&+ (\,-7\,644\,800\,\pi^6 - 38\,869\,488\,\pi^4 - 239\,621\,760\,(\zeta(3))^2 \\
&+ 18\,258\,549\,120\,\zeta(5) + 8\,937\,205\,200\,\zeta(3) + 18\,703\,515\,600\,\zeta(7) \\
&+ 7\,652\,120\,175\,)\,r^2 + (\,24\,601\,600\,\pi^6 + 115\,422\,048\,\pi^4 \\
&- 1\,158\,796\,800\,(\zeta(3))^2 - 61\,208\,904\,960\,\zeta(5) - 31\,040\,074\,800\,\zeta(3) \\
&- 74\,333\,972\,160\,\zeta(7) - 22\,632\,738\,975\,)\,r - 30\,086\,400\,\pi^6 \\
&- 131\,201\,280\,\pi^4 + 4\,882\,913\,280\,(\zeta(3))^2 + 80\,048\,424\,960\,\zeta(5) \\
&+ 39\,934\,581\,120\,\zeta(3) + 114\,181\,462\,080\,\zeta(7) + 24\,978\,502\,080\Big] \\
&+ \frac{{g_2}^5}{122\,880}\Big[(-1200\,\zeta(5) + 480\,\zeta(3) - 1005)\,r^4 \\
&+ \Big(-32\,\pi^4 + 19\,200\,\zeta(5) + 4320\,\zeta(3) + 26\,790\Big) r^3
\end{aligned}
$$

$$
\begin{aligned}
&+\left(560\pi^4-243\,600\,\zeta(5)-178\,080\,\zeta(3)-291\,090\right)r^2\\
&+\left(-2432\pi^4+1\,252\,800\,\zeta(5)+901\,920\,\zeta(3)+1\,033\,915\right)r\\
&+3776\pi^4-2\,395\,200\,\zeta(5)-1\,488\,960\,\zeta(3)-1\,364\,560\Big]\\
&+\frac{{g_2}^4 g_1}{1280}\Big[\left(4\pi^4-1000\,\zeta(5)-950\,\zeta(3)-1245\right)r^3\\
&+\left(-33\pi^4+11\,500\,\zeta(5)+9305\,\zeta(3)+10\,745\right)r^2\\
&+\left(160\pi^4-71\,800\,\zeta(5)-49\,745\,\zeta(3)-51\,255\right)r\\
&-216\pi^4+124\,800\,\zeta(5)+76\,800\,\zeta(3)+68\,110\Big]\\
&+\frac{{g_2}^3 {g_1}^2}{15\,360}\Big[\left(8\pi^4+360\,\zeta(3)+900\right)r^4+\left(-56\pi^4+6120\,\zeta(3)-4610\right)r^3\\
&+\left(1200\pi^4-336\,000\,\zeta(5)-288\,600\,\zeta(3)-271\,255\right)r^2\\
&+\left(-3632\pi^4+1\,560\,000\,\zeta(5)+1\,077\,000\,\zeta(3)+1\,014\,995\right)r\\
&+5296\pi^4-3\,100\,800\,\zeta(5)-1\,887\,360\,\zeta(3)-1\,526\,580\Big]\\
&+\frac{{g_2}^2 {g_1}^3}{15\,360}\Big[(1080\,\zeta(3)-400)\,r^5+(-2700\,\zeta(3)+495)\,r^4\\
&+\left(272\pi^4-19\,200\,\zeta(5)-46\,080\,\zeta(3)-23\,830\right)r^3\\
&+\left(-664\pi^4+67\,200\,\zeta(5)+118\,620\,\zeta(3)+75\,465\right)r^2\\
&+\left(3432\pi^4-1\,737\,600\,\zeta(5)-1\,080\,840\,\zeta(3)-947\,210\right)r\\
&-4720\pi^4+2\,755\,200\,\zeta(5)+1\,686\,720\,\zeta(3)+1\,335\,280\Big]\\
&+\frac{g_2 {g_1}^4}{20\,480}\Big[(240\,\zeta(3)-145)\,r^6+(-720\,\zeta(3)+435)\,r^5\\
&+\left(32\pi^4-5040\,\zeta(3)-715\right)r^4+\left(-64\pi^4+11\,280\,\zeta(3)+705\right)r^3\\
&+\left(576\pi^4-201\,600\,\zeta(5)-140\,160\,\zeta(3)-139\,440\right)r^2\\
&+(\,-544\pi^4+201\,600\,\zeta(5)+134\,400\,\zeta(3)+139\,160\,)\,r\\
&+2880\pi^4-1\,747\,200\,\zeta(5)-1\,088\,640\,\zeta(3)-787\,160\Big].
\end{aligned}
\tag{50}
$$

$$
\beta_{\lambda_m}=2\,(1-\varepsilon)\lambda_m+H_{mn}\lambda_n \tag{51}
$$

$$
\begin{aligned}
H_{11} = &-\frac{{g_1}^3}{512}\Big[-543\,r^4+1086\,r^3+(-6528\,\zeta\,(3)-22\,995)\,r^2+(6528\,\zeta\,(3)+22\,452)\,r\\
&-45\,312\,\zeta\,(3)-120\,780\Big]\\
&-\frac{g_2{g_1}^2}{256}\Big[-1629r^3-16\,128\zeta\,(3)\,r+3258r^2+16\,128\zeta\,(3)-44\,019r+42\,390\Big]\\
&-\frac{{g_1}^2}{16}\Big[81\,r^2-81\,r+594\Big]\\
&-\frac{g_1{g_2}^2}{1024}\Big[-9\,r^4+36\,r^3+(-3456\,\zeta\,(3)-19\,041)\,r^2\\
&+(10\,368\,\zeta\,(3)+42\,978)\,r-69\,120\,\zeta\,(3)-142\,728\Big]\\
&-\frac{63}{4}\,[r-1]\,g_1g_2-\frac{{g_2}^3}{512}\Big[-93\,r^3+498\,r^2\\
&+(-3456\,\zeta\,(3)-7833)\,r+6912\,\zeta\,(3)+11\,856\Big]\\
&-{g_2}^2\frac{9}{32}\Big[r^2-3\,r+28\Big]+\frac{3}{2}\,[r-1]\,g_2+\frac{3}{4}\Big[r^2-r+14\Big]\,g_1;
\end{aligned}
$$

$$
\begin{aligned}
H_{12} = &-\frac{1}{64}\Big[-130\,r^3+260\,r^2+(-768\,\zeta\,(3)-3311)\,r+768\,\zeta\,(3)+3181\Big]\,{g_1}^3\\
&-\frac{1}{512}\,g_2{g_1}^2\Big[-66\,548-576\,\zeta\,(3)\,r^2+1728\,\zeta\,(3)\,r-3\,r^4+12\,r^3\\
&-19\,584\,\zeta\,(3)+18\,178\,r-8363\,r^2\Big]\\
&-\frac{11}{2}\,[r-1]\,{g_1}^2-\frac{3}{8}\,g_2g_1\Big[r^2-3\,r+30\Big]-[1-r]\,g_1-\frac{9}{8}\,[r-2]\,{g_2}^2+\frac{3}{2}\,g_2\\
&-\frac{{g_2}^2g_1}{256}\Big[-105\,r^3-2304\,\zeta\,(3)\,r+564\,r^2+4608\,\zeta\,(3)-10\,227\,r+15\,534\Big]\\
&-\frac{{g_2}^3}{256}\Big[-96\,\zeta\,(3)\,r^2+576\,\zeta\,(3)\,r-217\,r^2-2400\,\zeta\,(3)+999\,r-4203\Big]\,{g_2}^3;
\end{aligned}
$$

$$
\begin{aligned}
H_{13} = &\frac{3}{4}\,g_1+\frac{9}{8}\,[2-r]\,g_2g_1\\
&-\frac{33}{8}\,{g_1}^2-\frac{45}{32}\,{g_2}^2+\frac{{g_1}^3}{512}\Big[19\,794+4608\,\zeta\,(3)-4143\,r+2019\,r^2\Big]\\
&+\frac{g_2{g_1}^2}{512}\Big[18\,r^3-81\,r^2+(1728\,\zeta\,(3)+16\,953)\,r-3456\,\zeta\,(3)-27\,744\Big]\\
&+\frac{{g_2}^2g_1}{1024}\Big[2367\,r^2+9216\,\zeta\,(3)-11\,097\,r+49\,992\Big]\\
&+\frac{{g_2}^3}{512}\,[(480\,\zeta\,(3)+1731)\,r-1776\,\zeta\,(3)-4956];
\end{aligned}
$$

$$
\begin{aligned}
H_{21} = {} & \frac{g_2 {g_1}^2}{128}\left[(-864\,\zeta\,(3)-5427)\,r^2+(864\,\zeta\,(3)+5427)\,r-25\,920\,\zeta\,(3)-69\,390\right]\\
& +\frac{{g_2}^2 g_1}{256}\left[-258r^3+903r^2+(-16\,128\zeta\,(3)-49\,293)\,r+29\,952\zeta\,(3)+75\,072\right]\\
& +\frac{9}{4}\left[r^2-r+26\right]g_2 g_1\\
& +\frac{{g_2}^3}{256}\left[(-576\,\zeta\,(3)-1659)\,r^2+(3456\,\zeta\,(3)+7227)\,r-13\,824\,\zeta\,(3)-28\,686\right]\\
& +\frac{9}{4}\left[-7+4\,r\right]{g_2}^2-9\,g_2;
\end{aligned}
$$

$$
\begin{aligned}
H_{22} = {} & \frac{{g_1}^3}{512}\Big[-23\,r^4-3456\zeta\,(3)\,r^2+46\,r^3+3456\,\zeta\,(3)\,r-8711r^2\\
& -39\,168\zeta\,(3)+8688r-95\,332\Big]\\
& +\frac{g_2 {g_1}^2}{256}\left[73\,808-17\,280\,\zeta\,(3)\,r-583\,r^3+25\,920\,\zeta\,(3)-49\,392\,r+1793\,r^2\right]\\
& +\frac{{g_1}^2}{16}\left[37\,r^2-37\,r+506\right]+\frac{3}{4}\left[-36+23\,r\right]g_2 g_1+\frac{3}{32}\left[5\,r^2-27\,r+188\right]{g_2}^2\\
& +\frac{{g_2}^2 g_1}{1024}\Big[-341\,344-4224\zeta\,(3)\,r^2+21\,888\zeta\,(3)\,r-3\,r^4+12\,r^3\\
& -132\,096\,\zeta\,(3)+84\,730r-21\,871r^2\Big]+\frac{{g_2}^3}{512}\Big[-115\,r^3+(192\,\zeta\,(3)+1144)\,r^2\\
& +(-5760\,\zeta\,(3)-20\,269)\,r+17\,472\,\zeta\,(3)+46\,094\Big]\\
& +\frac{g_1}{4}\left[-r^2+r-38\right]+\frac{3}{2}\left[2-r\right]g_2;
\end{aligned}
$$

$$
\begin{aligned}
H_{23} = {} & \frac{3}{4}\left[2\,r-3\right]g_1+\frac{9}{2}\,g_2+\frac{9}{16}\,g_1 g_2\left[-r^2+5\,r-56\right]\\
& +\frac{{g_1}^3}{512}\left[498\,r^3-1245\,r^2+(9216\,\zeta\,(3)+34\,671)\,r-13\,824\,\zeta\,(3)-50\,886\right]\\
& +\frac{g_2 {g_1}^2}{256}\left[432\zeta\,(3)\,r^2-2160\zeta\,(3)\,r+6081r^2+27\,648\zeta\,(3)-22\,191r+85\,194\right]\\
& +\frac{33}{8}\,{g_1}^2\left[3-2\,r\right]+\frac{g_1 {g_2}^2}{1024}\Big[630\,r^3+29\,952\,\zeta\,(3)\,r-5751\,r^2\\
& -87\,552\,\zeta\,(3)+118\,875\,r-273\,816\Big]+\frac{1}{512}\Big[432\,\zeta\,(3)\,r^2-4176\,\zeta\,(3)\,r\\
& +1791\,r^2+18\,000\,\zeta\,(3)-13\,872\,r+46\,488\Big]{g_2}^3;
\end{aligned}
$$

$$
\begin{aligned}
H_{31} = {} & \frac{27}{128}\,{g_2}^2 g_1\left[-1304-384\,\zeta\,(3)+43\,r-43\,r^2\right]+\frac{27}{2}\,{g_2}^2\\
& +\frac{3}{32}\,{g_2}^3\left[1074-32\,\zeta\,(3)\,r+224\,\zeta\,(3)-435\,r\right]
\end{aligned}
$$

$$
\begin{aligned}
H_{32} = {} & \frac{g_2 {g_1}^2}{32}\left[3r^4 - 72\zeta(3)\,r^2 - 6r^3 + 72\zeta(3)\,r - 351r^2 - 4032\zeta(3) + 354r - 9261\right] \\
& + \frac{g_1 {g_2}^2}{128}\left[40\,150 - 5376\,\zeta(3)\,r - 43\,r^3 + 15\,168\,\zeta(3) - 16\,145\,r + 344\,r^2\right] \\
& + \frac{3}{4}\,g_2 g_1\left[r^2 - r + 48\right] - 6\,g_2 \\
& + \frac{{g_2}^2}{256}\Big(-288\,\zeta(3)\,r^2 + 2592\,\zeta(3)\,r - 1313\,r^2 - 11\,520\,\zeta(3) \\
& + 10\,245\,r - 33\,140\Big){g_2}^3 + 3/4\,(-23 + 8\,r)\,;
\end{aligned}
$$

$$
\begin{aligned}
H_{33} = {} & \frac{{g_1}^3}{256}\left[-30\,r^4 + 60\,r^3 + (960\,\zeta(3) + 1155)\,r^2 + (-960\,\zeta(3) - 1185)\,r\right. \\
& \left. + 13\,440\,\zeta(3) + 25\,050\right] \\
& + \frac{{g_1}^2 g_2}{256}\left[-49\,r^3 - 55\,r^2 + (5376\,\zeta(3) + 11\,266)\,r - 12\,864\,\zeta(3) - 27\,368\right] \\
& + \frac{15}{2}\,g_1 + \frac{15}{16}\,{g_1}^2\left[-r^2 + r - 22\right] + \frac{9}{4}\,g_2 g_1\,[18 - 7\,r] + \frac{3}{2}\,[r - 4]\,g_2 \\
& + \frac{9}{16}\left[-r^2 + 10\,r - 42\right]{g_2}^2 + \frac{{g_2}^2 g_1}{512}\left[(2304\,\zeta(3) + 8115)\,r^2.\right. \\
& \left. + (-21\,888\,\zeta(3) - 63\,753)\,r + 87\,552\,\zeta(3) + 200\,436\right] \\
& + \frac{{g_2}^3}{512}\left[126\,r^3 + (-432\,\zeta(3) - 2607)\,r^2 + (7536\,\zeta(3) + 26\,949)\,r\right. \\
& \left. - 25\,536\,\zeta(3) - 69\,336\right].
\end{aligned}
$$

References

[1] A.A. Abrikosov, L.P. Gorkov, I.E. Dzyaloshinski, Methods of Quantum Field Theory in Statistical Physics, Dobrosvet, Moscow, 2006.
[2] A.N. Vasil'ev, Functional Methods in Quantum Field Theory and Statistical Physics, Gordon and Breach, Amsterdam, 1998.
[3] M.A. Baranov, M.Yu. Kagan, Yu. Kagan, JETP Lett. 64 (4) (1996) 273.
[4] R.W. Cherng, G. Refael, E. Demler, Phys. Rev. Lett. 99 (2007) 130406.
[5] Tomoki Ozawa, Gordon Baym, Phys. Rev. A 82 (2010) 063615.
[6] John L. Bohn, Phys. Rev. A 61 (2000) 053409.
[7] Congjun Wu, Physics 3 (2010) 92.
[8] Tin-Lun Ho, Sungkit Yip, Phys. Rev. Lett. 82 (2) (1999) 247.
[9] Miguel A. Cazalilla, arXiv:1403.2792v1, 2014.
[10] Masaru Sakaida, Norio Kawakami, Phys. Rev. A 90 (2014) 013632.
[11] M.A. Cazalilla, A.F. Ho, M. Ueda, New J. Phys. 11 (2009) 103033.
[12] M.I. Katsnelson, Graphene. Carbon in Two Dimensions, Camdridge University Press, 2012.
[13] L.P. Gor'kov, T.K. Melik-Barkhudarov, J. Exp. Theor. Phys. 40 (1961) 1452.
[14] J. Honkonen, M.V. Komarova, M.Yu. Nalimov, Theor. Math. Phys. 176 (1) (2013) 89.
[15] G.A. Kalagov, M.V. Kompaniets, M.Yu. Nalimov, Theor. Math. Phys. 181 (2) (2014) 1448.
[16] A.N. Vasil'ev, Quantum-Field Renormalization Group in the Critical Behavior Theory and in Stochastic Dynamics, St. Petersburg Institute for Nuclear Physics, St. Petersburg, 1998.
[17] L.N. Lipatov, J. Exp. Theor. Phys. 72 (1977) 411.

[18] J.A.M. Vermaseren, New features of FORM, arXiv:math-ph/0010025.
[19] K.G. Chetyrkin, A.L. Kataev, F.V. Tkachev, Phys. Lett. B 99 (1981) 147, Errata: Phys. Lett. B 101 (1981) 457;
K.G. Chetyrkin, S.G. Gorishny, S.A. Larin, F.V. Tkachov, Phys. Lett. B 132 (1983) 351;
D.I. Kazakov, Phys. Lett. B 133 (6) (1983) 406;
D.I. Kazakov, Theor. Math. Phys. 58 (1984) 223;
D.I. Kazakov, Teor. Mat. Fiz. 58 (3) (1984) 343;
K.G. Chetyrkin, S.G. Gorishny, S.A. Larin, F.V. Tkachov, preprint INR P-0453, Moscow, 1986;
H. Kleinert, J. Neu, V. Shulte-Frohlinde, K.G. Chetyrkin, S.A. Larin, Phys. Lett. B 272 (1991) 39, Erratum: Phys. Lett. B 319 (1993) 545.
[20] L. Ts. Adzhemyan, M.V. Kompaniets, J. Phys. Conf. Ser. 523 (2014) 012049.
[21] J. Honkonen, M.V. Komarova, M.Yu. Nalimov, Nucl. Phys. B 714 (3) (2005) 292.
[22] M.V. Komarova, M.Yu. Nalimov, Theor. Math. Phys. 126 (3) (2001) 339.
[23] G.A. Kalagov, M.Yu. Nalimov, Nucl. Phys. B 884 (2014) 672.
[24] J. Zinn-Justin, Quantum Field Theory and Critical Phenomena, 3rd edition, Clarendon Press, Oxford, 1996.
[25] Hagen Kleinert, Verena Schulte-Frohlinde, Critical Properties of ϕ^4-Theories, World Scientific, Singapore, 2001.
[26] M.Yu. Nalimov, V.A. Sergeev, L. Sladkoff, Theor. Math. Phys. 159 (1) (2009) 96.